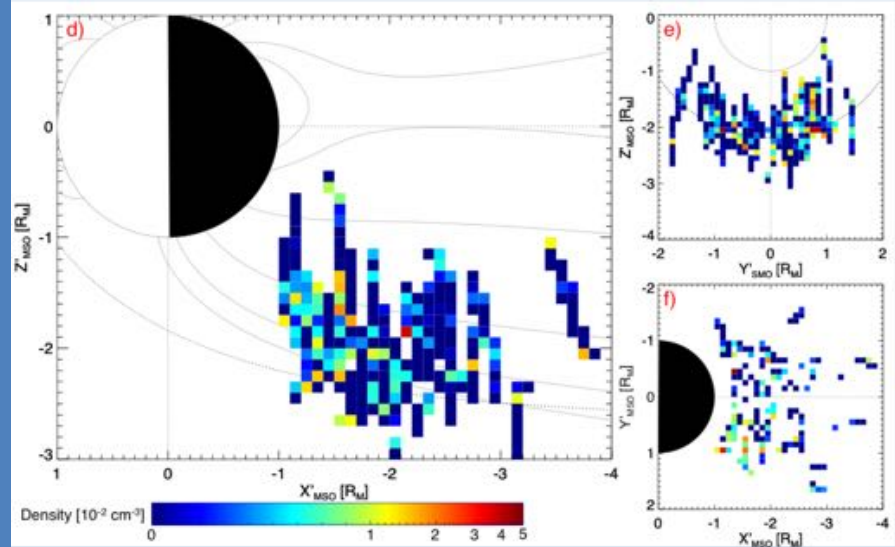


Magnetic Reconnection



Sodium Ion Mantle

MAGNETOSPHERE OF MERCURY: THE VIEW FROM MESSENGER

James A. Slavin

Department of Climate and Space Sciences & Engineering

University of Michigan

Planetary Magnetospheres

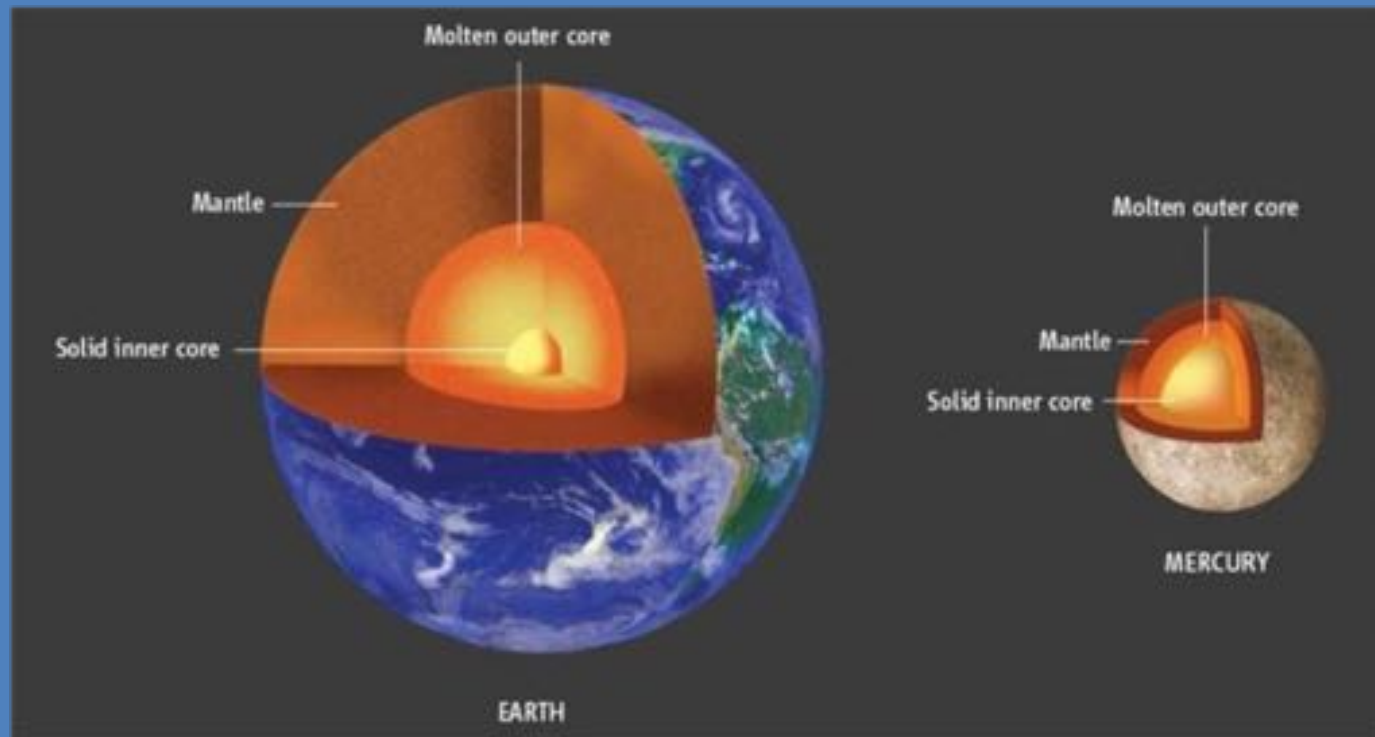
Lecture #1

Heliophysics Summer School

27 July 2018

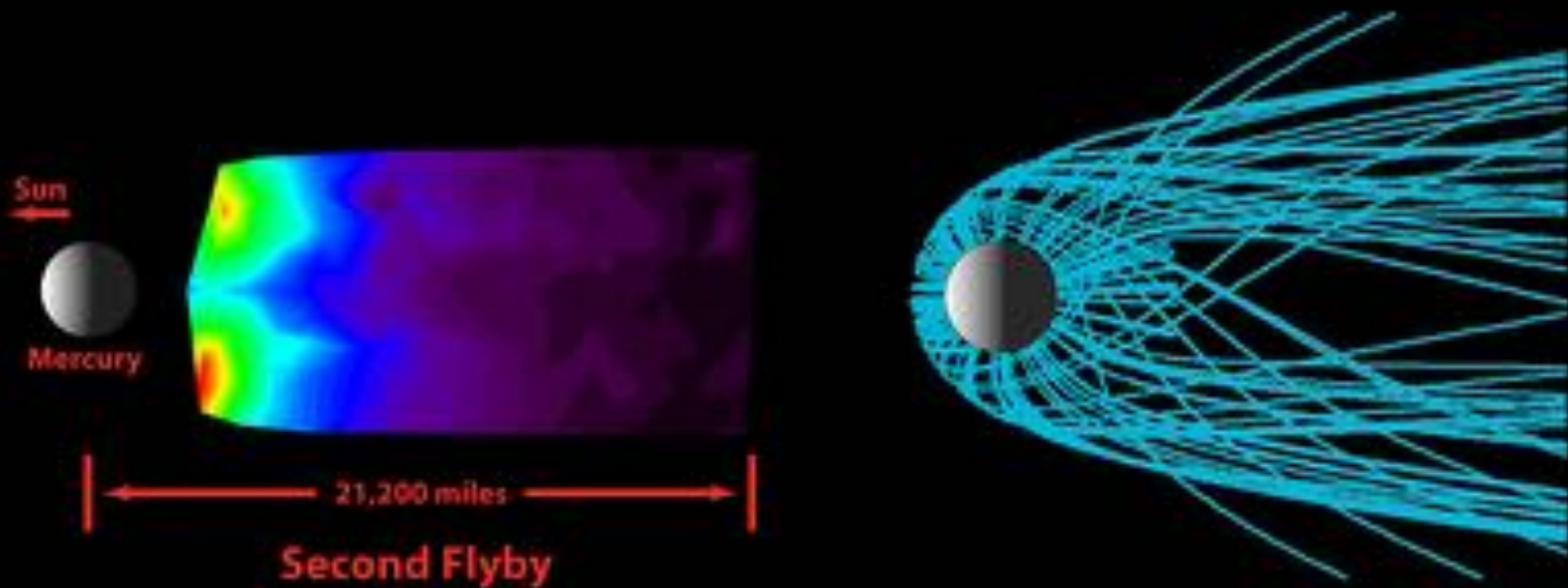
Boulder, Colorado

Earth and Mercury



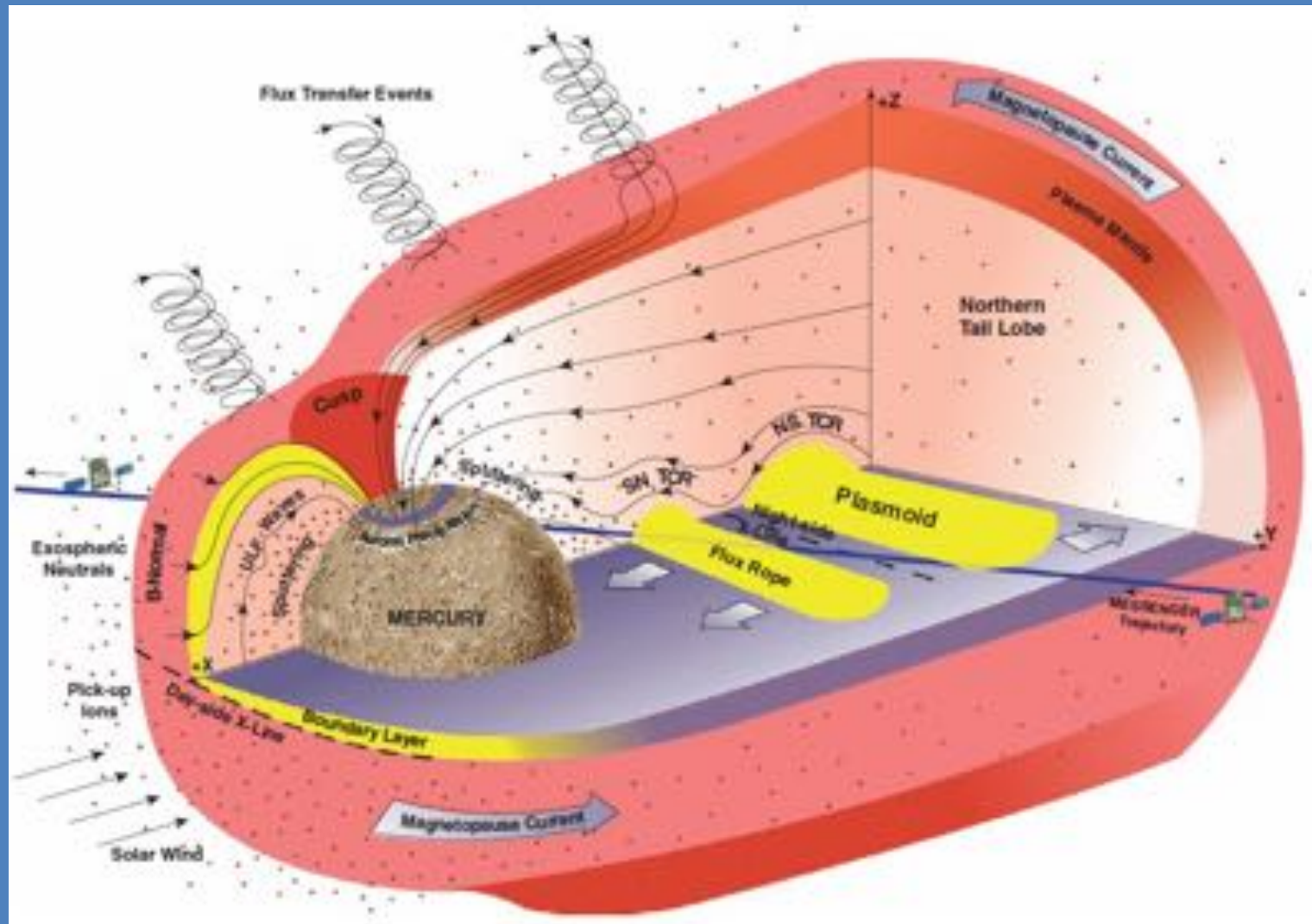
Equatorial B-Fields: 32,000 nT and 200 nT

High-Energy Release Coupled with Strong Radiation Pressure Produces an Extended Neutral Tail

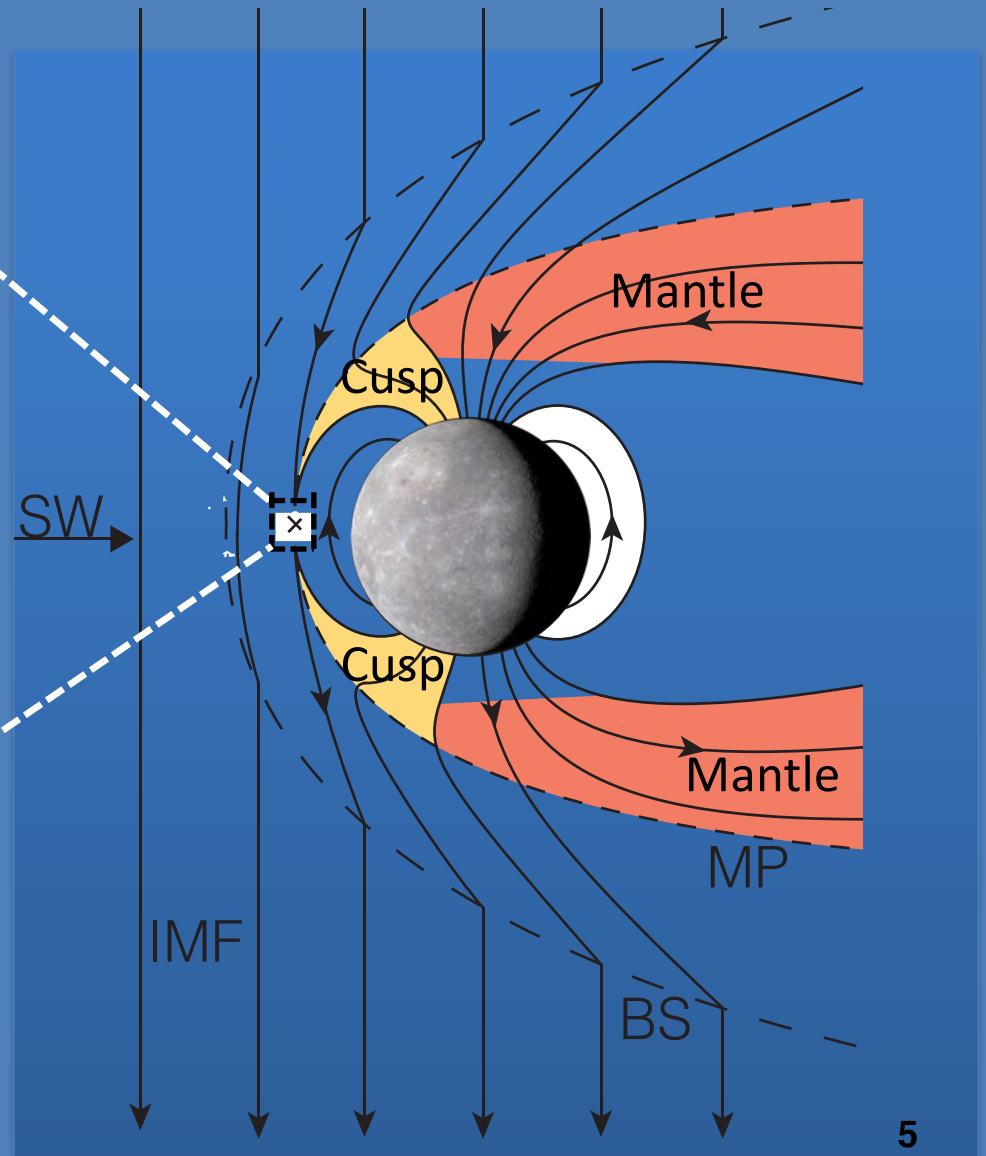
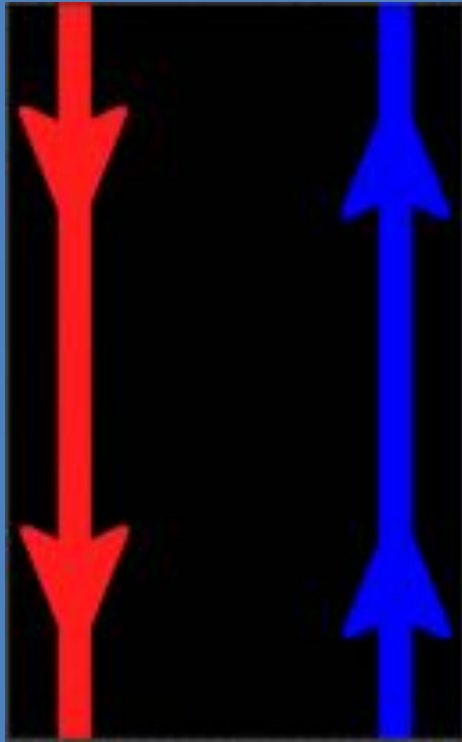


Courtesy R. Vervack

Mercury's Reconnection-Driven Magnetosphere

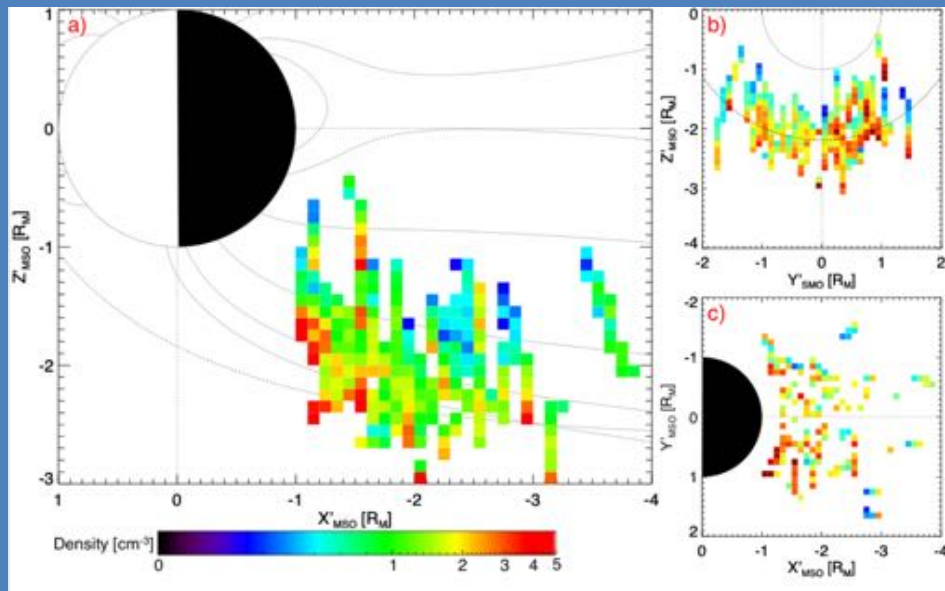


Magnetopause Reconnection



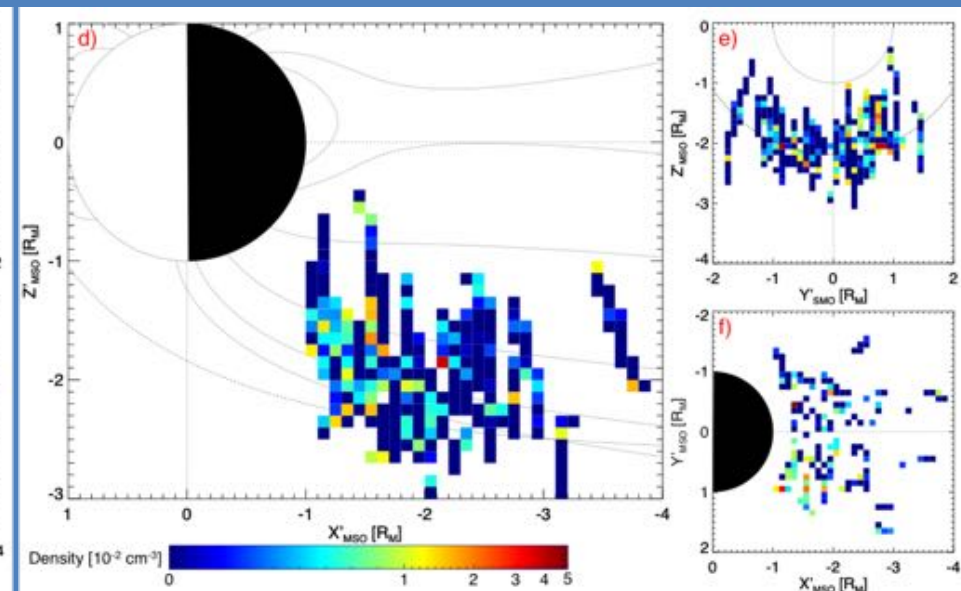
Reconnection and solar wind plasma entry in Mercury's Magnetosphere
Courtesy J. Jasinski (JPL/Caltech)

Ion Outflow - H^+ and Na^+ Plasma Mantle



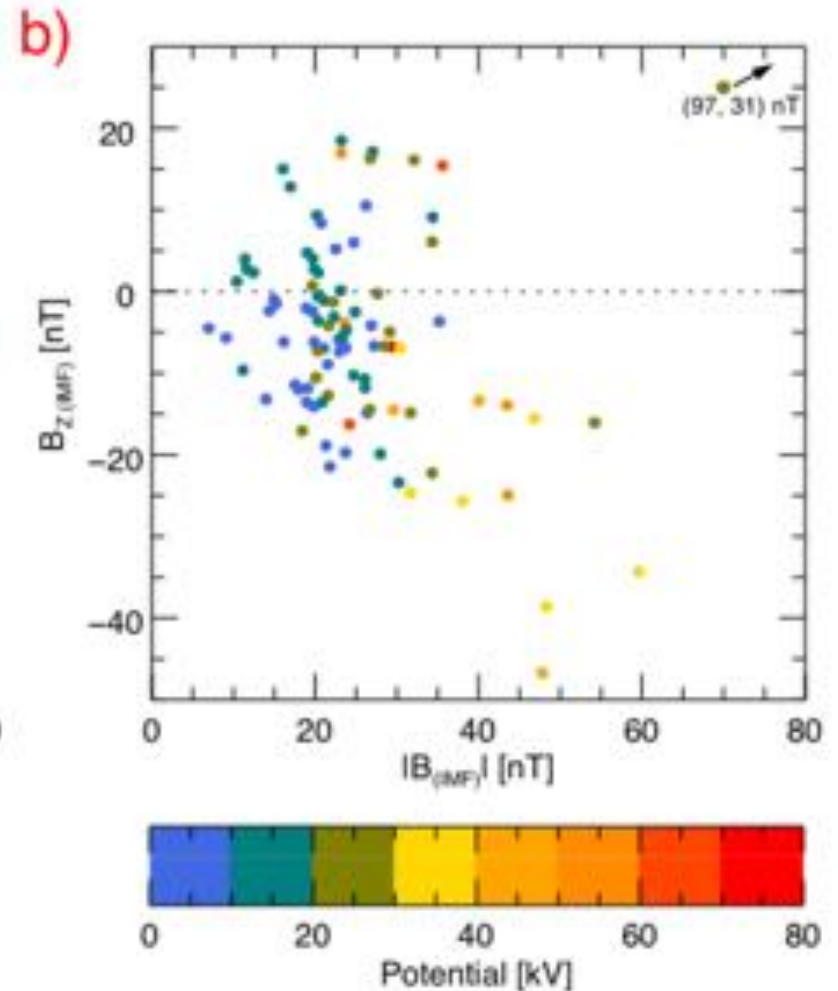
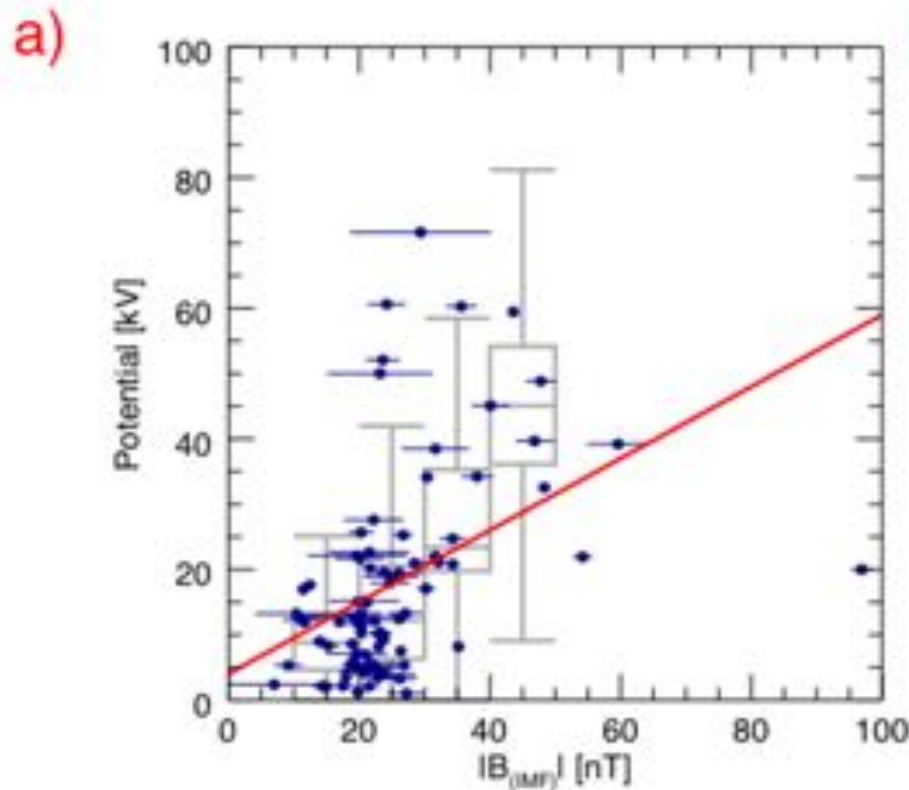
H^+ Ions

Jasinski et al. (2017)

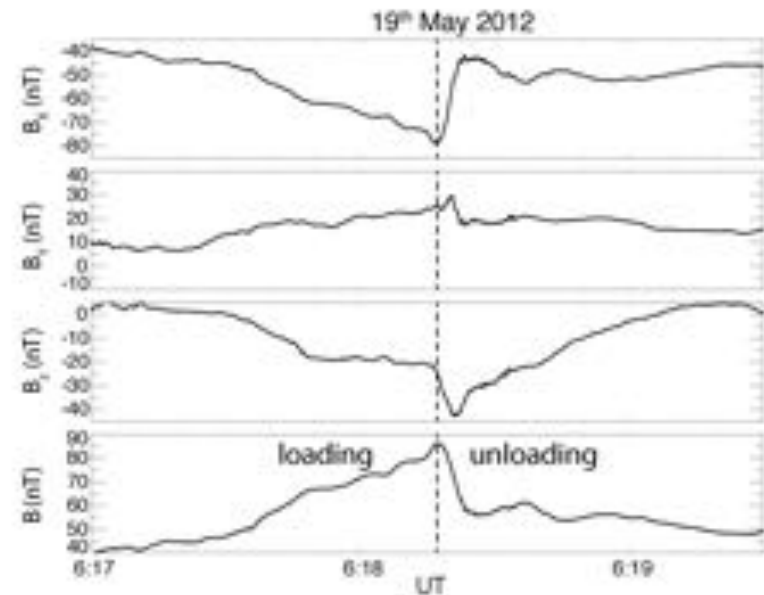
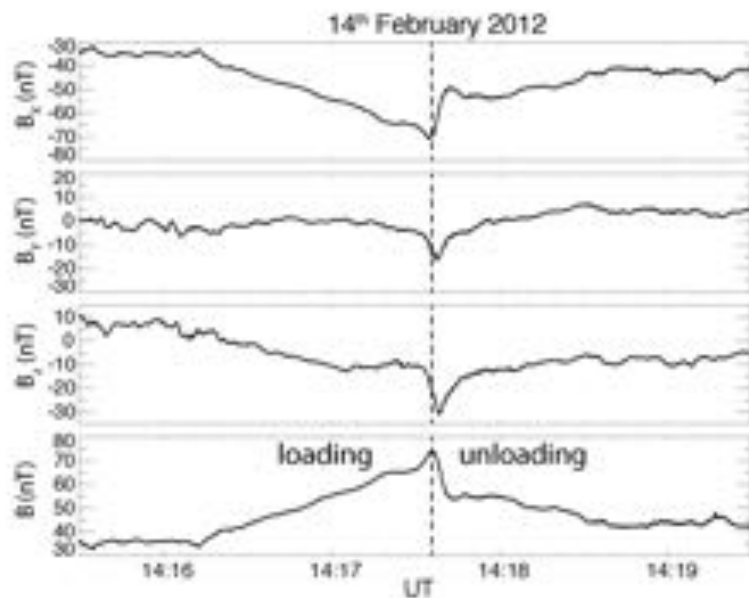


Na^+ Ions

Cross-Magnetosphere Electric Potential

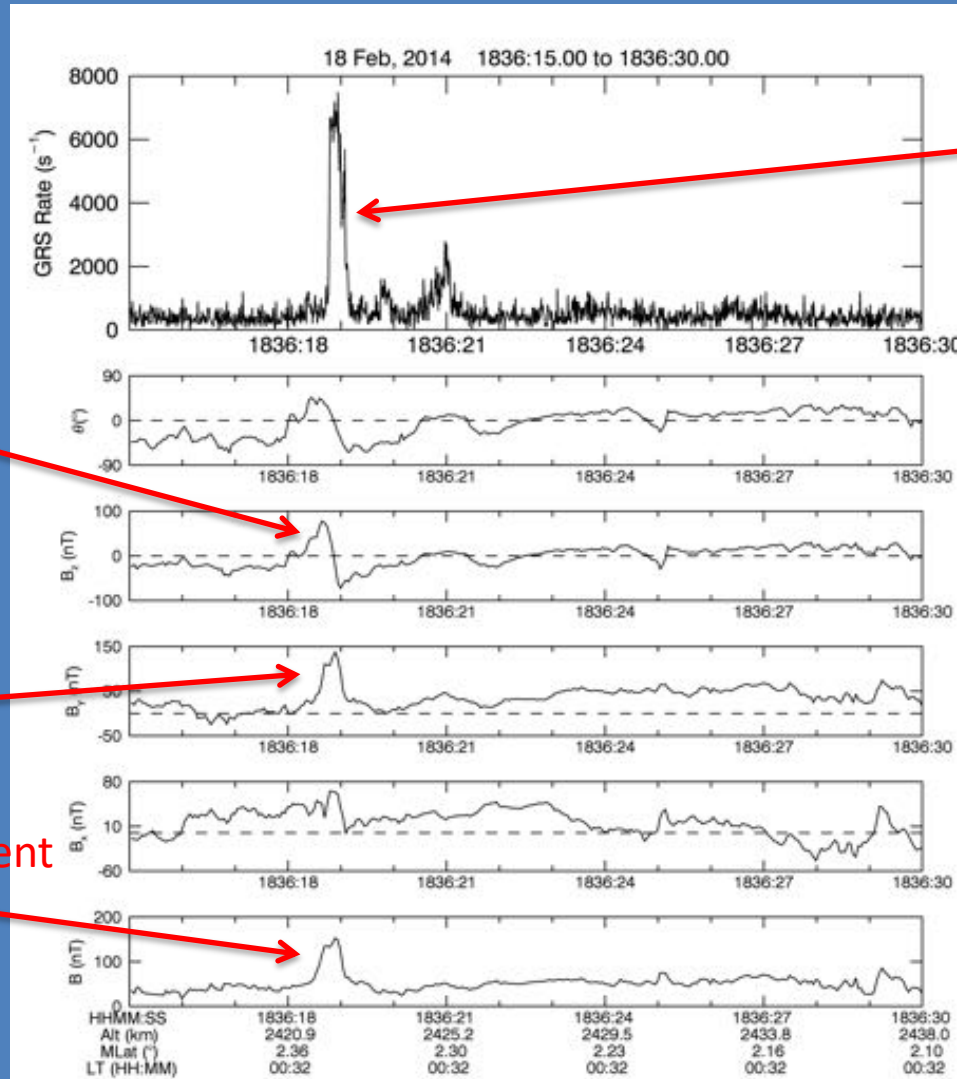


Substorms at Mercury: Extreme Loading – Unloading Events



Slavin et al. (*Mercury*, 2018)

Energetic Electrons in Cross-tail Current Sheet Flux Ropes at Mercury



bipolar in Bz

core field in By

total field enhancement

energetic e⁻!

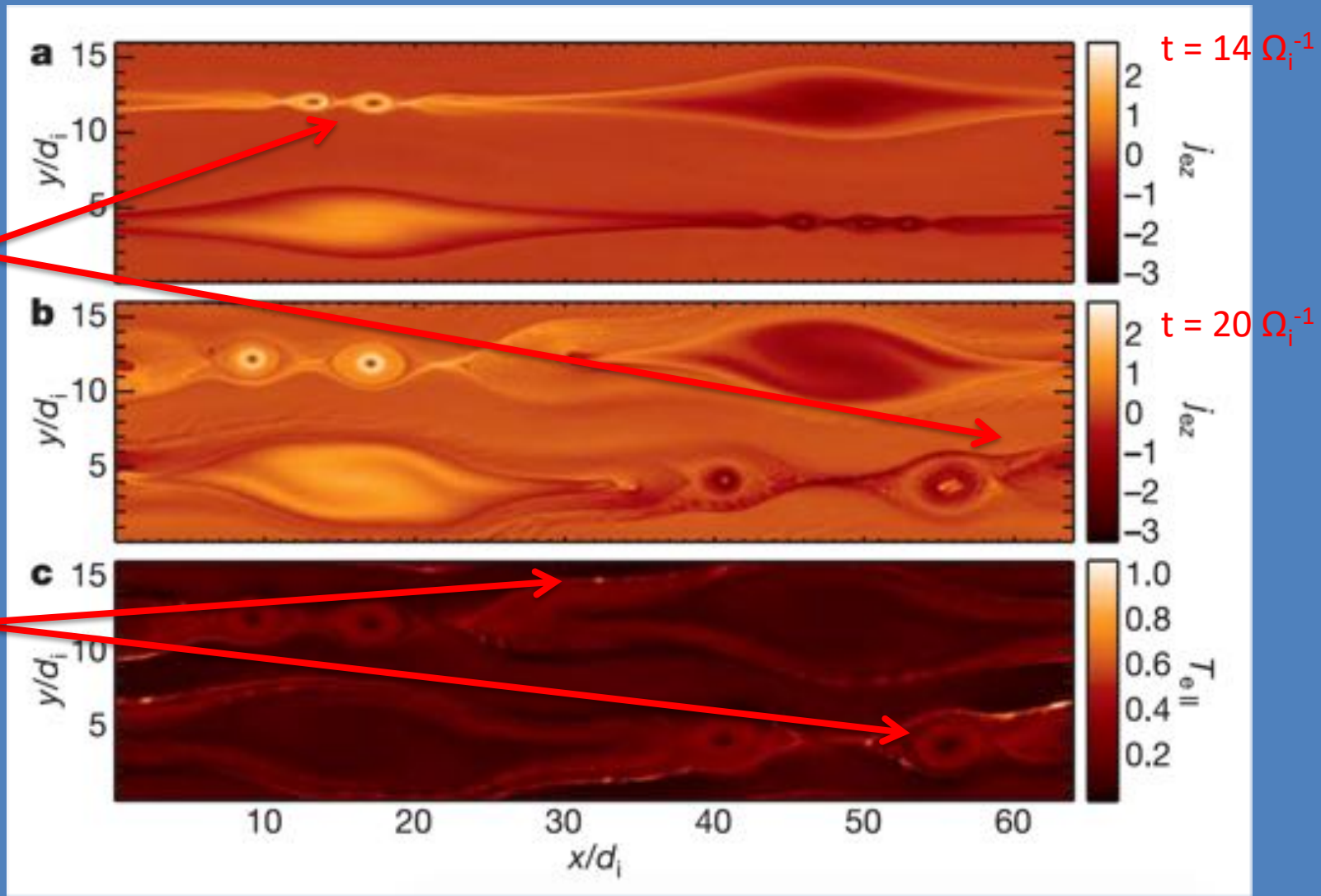
(observation of Fermi acceleration?)

Flux rope, tailward traveling!

Fermi Acceleration of Electrons in Coalescing Flux Ropes

formation,
growth,
merging of
secondary
magnetic
islands

heating
around
rims and
inside
islands



Flux Rope Coalescence and Energetic Electron Acceleration

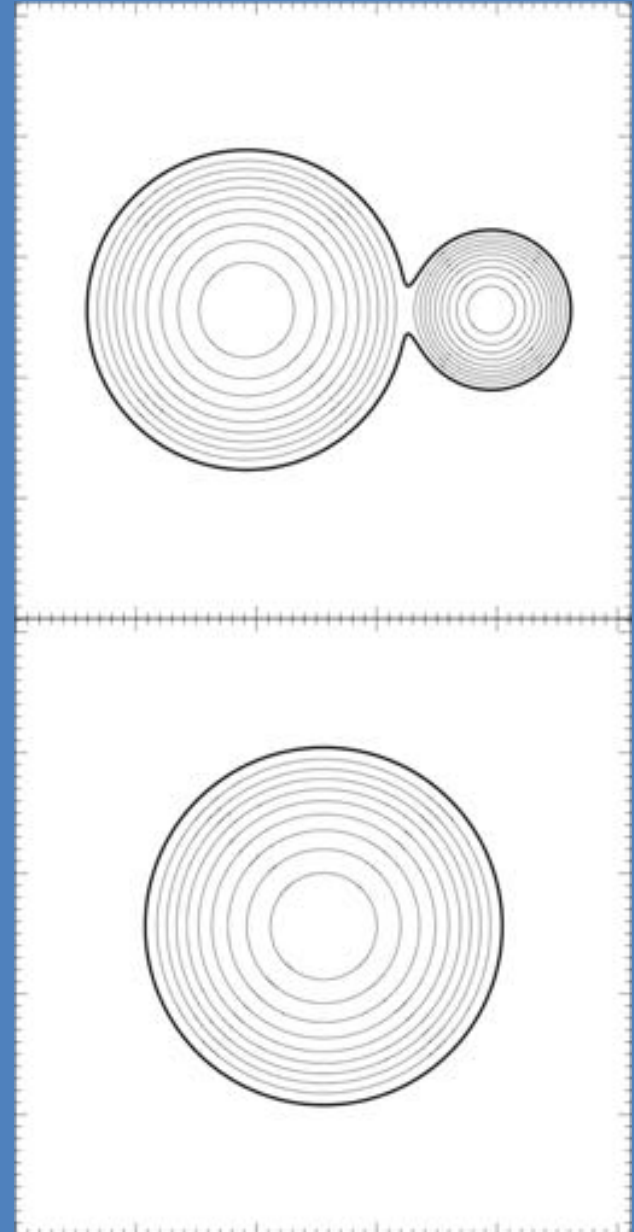
- Total area preserved
- Magnetic flux of largest island is preserved
- Particle conservation laws
 - Magnetic moment $\mu = p_{\perp}^2 / 2mB$
 - Parallel action $p_{\parallel} L$
 - Field line shortening drives energy gain

$$\frac{dp_{\parallel}^2}{dt} \sim 2 \frac{0.1c_A}{r_1 + r_2} p_{\parallel}^2$$

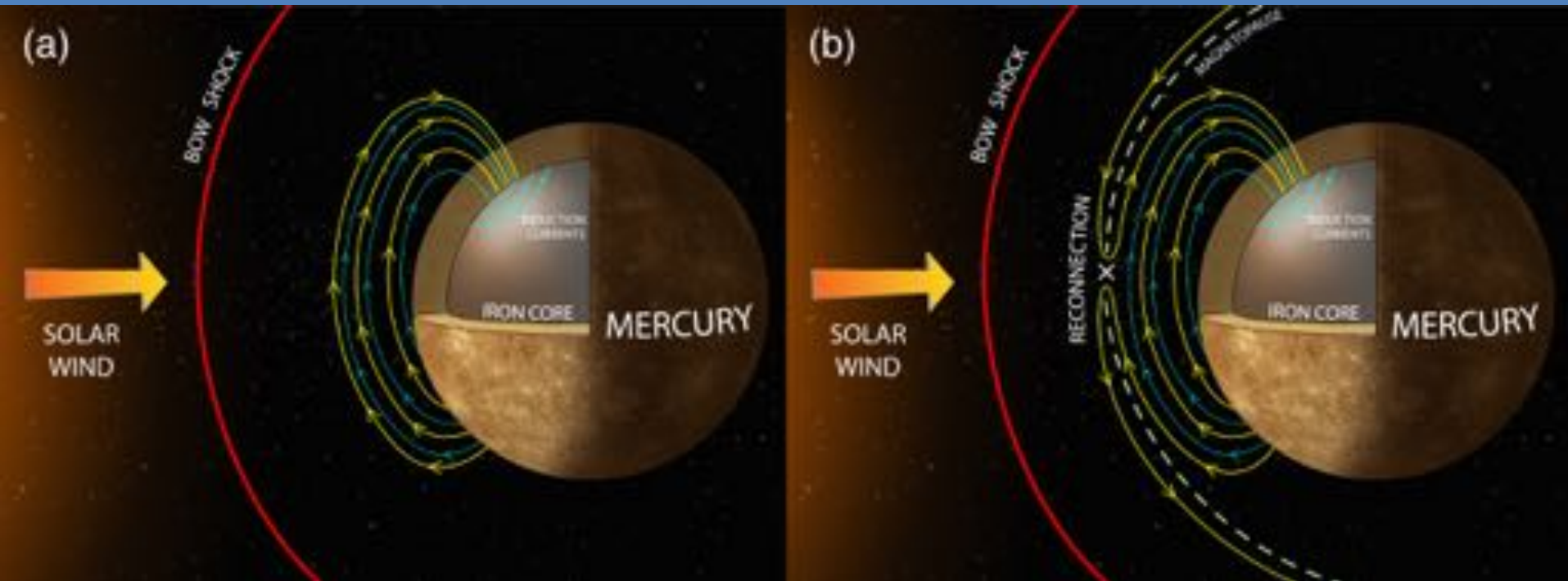
$$\frac{dp_{\perp}^2}{dt} \sim - \frac{0.1c_A}{r_1 + r_2} p_{\perp}^2$$

- No energy gain when isotropic

Courtesy of J. Drake



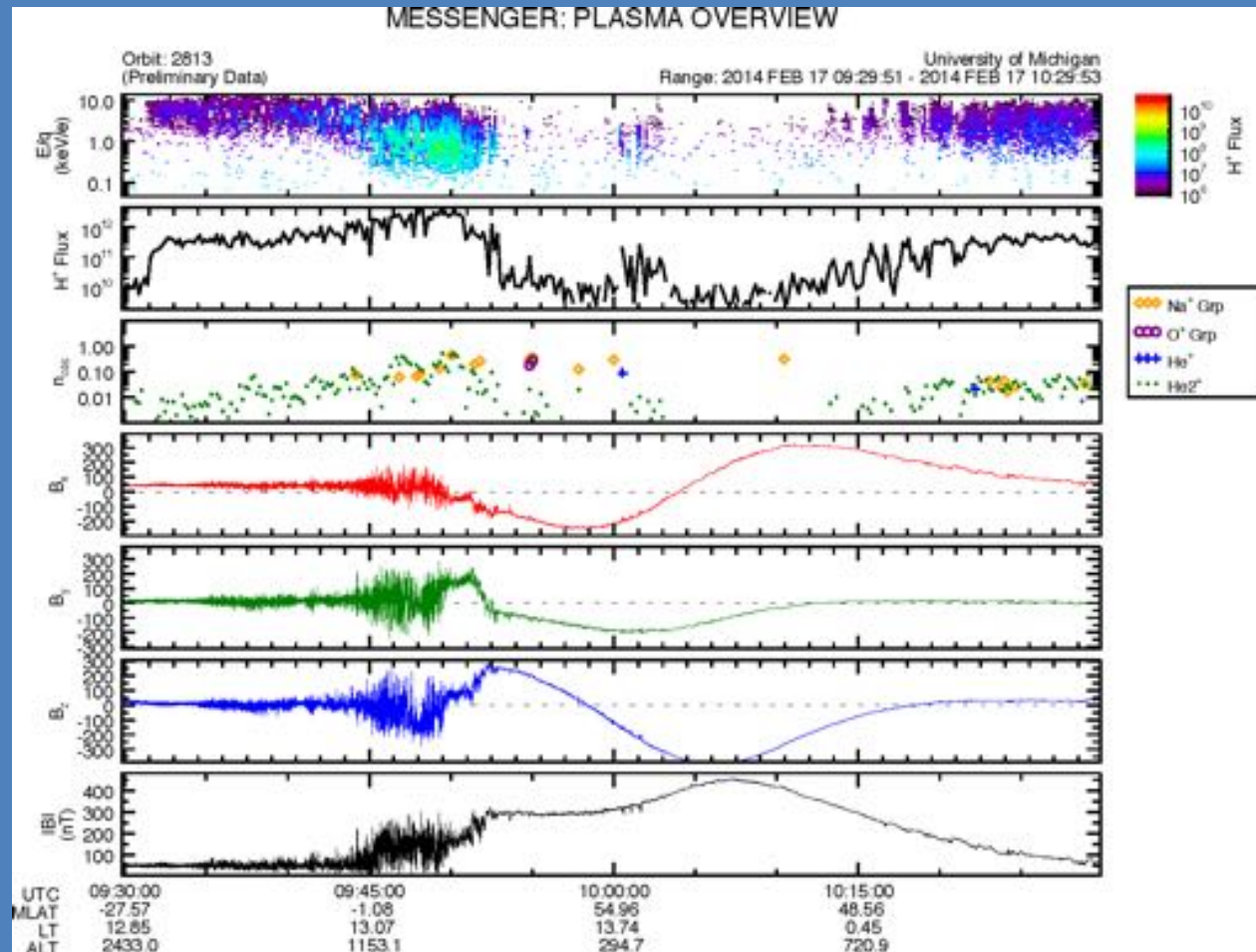
Solar Wind – Core Coupling



The harder the Solar Wind pushes ... the more induction currents add to Mercury's magnetic moment, but dayside magnetic reconnection has the opposite effect.

(Hood and Schubert, 1979; Slavin et al., 1979; 2014)

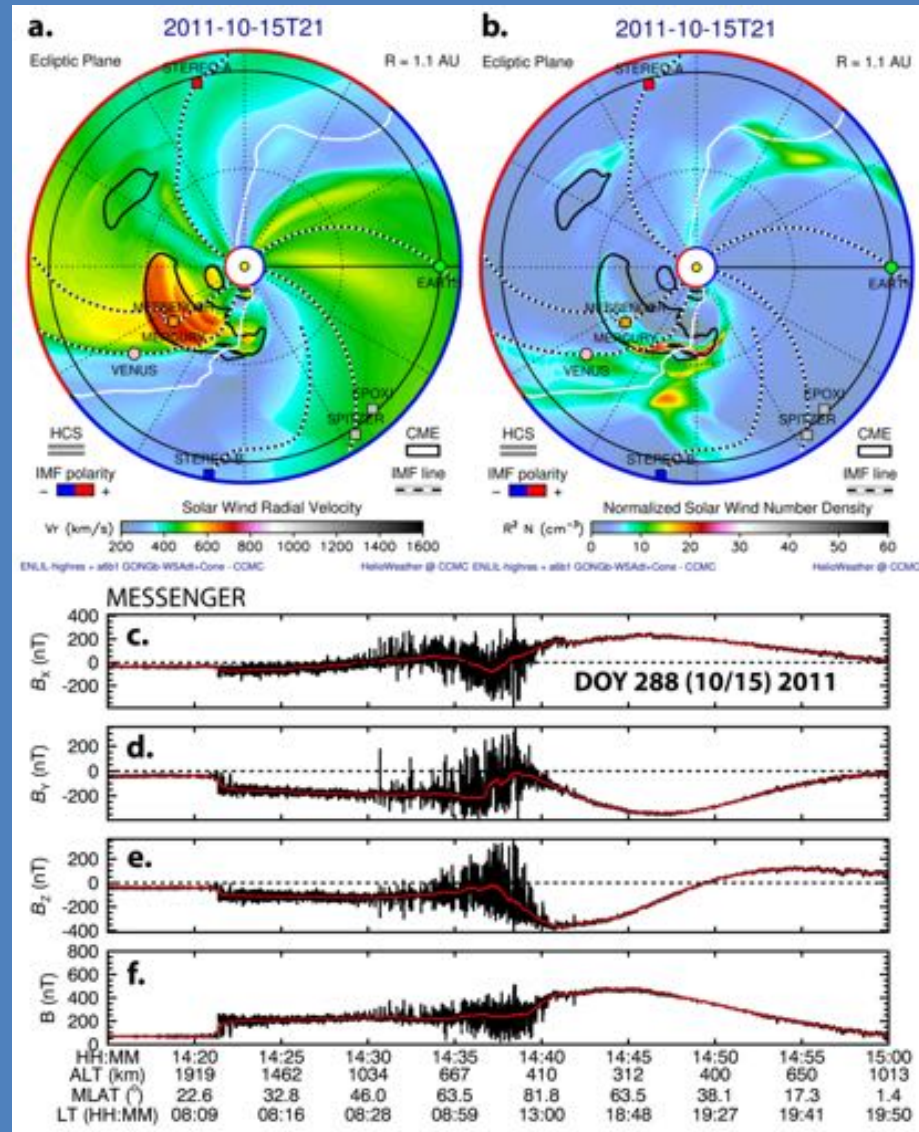
Highly Compressed Magnetosphere



Slavin et al. (2018)

$P_{sw} \sim 50 \text{ nPa}$

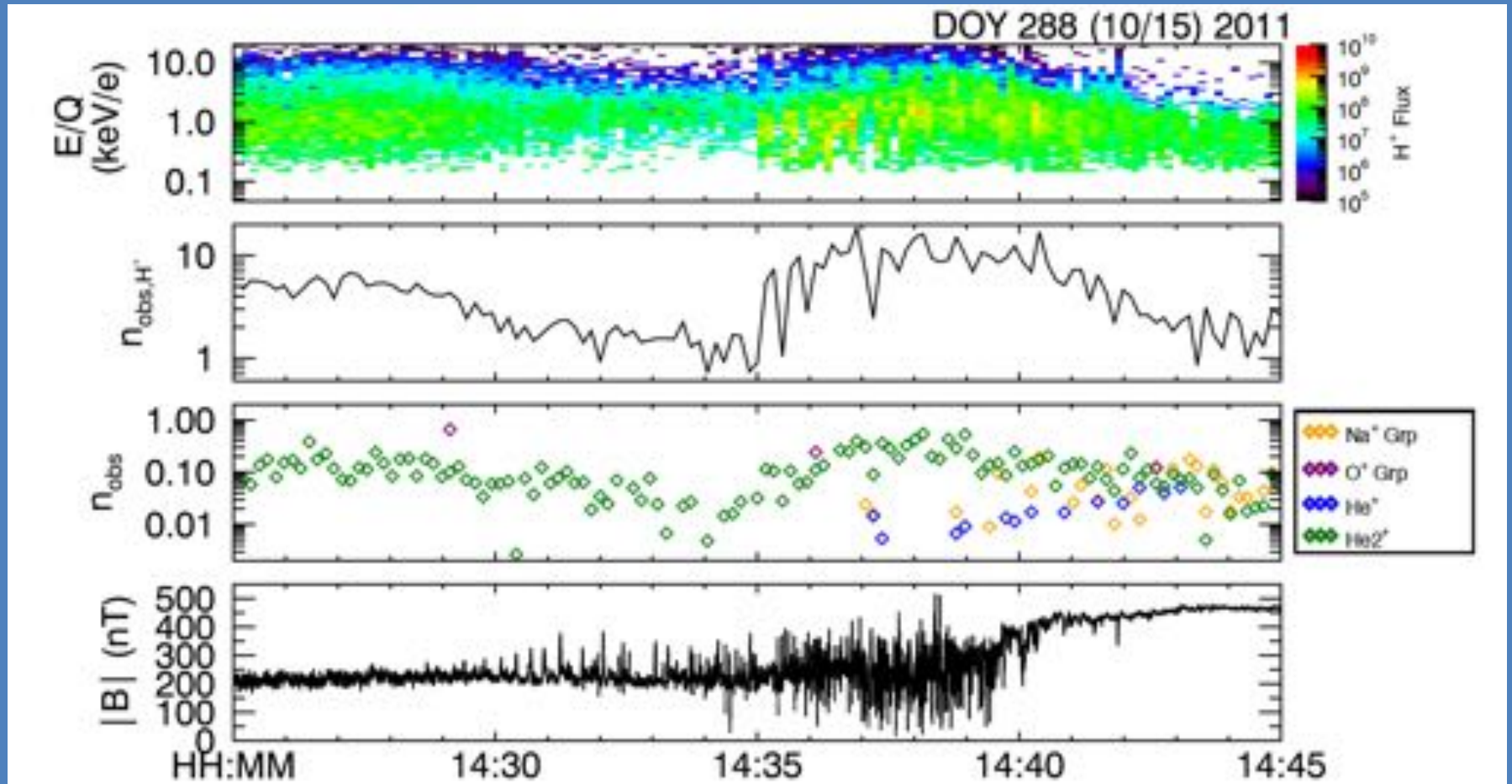
Disappearing Dayside Magnetosphere (DDM) Events



Slavin et al. (2018)

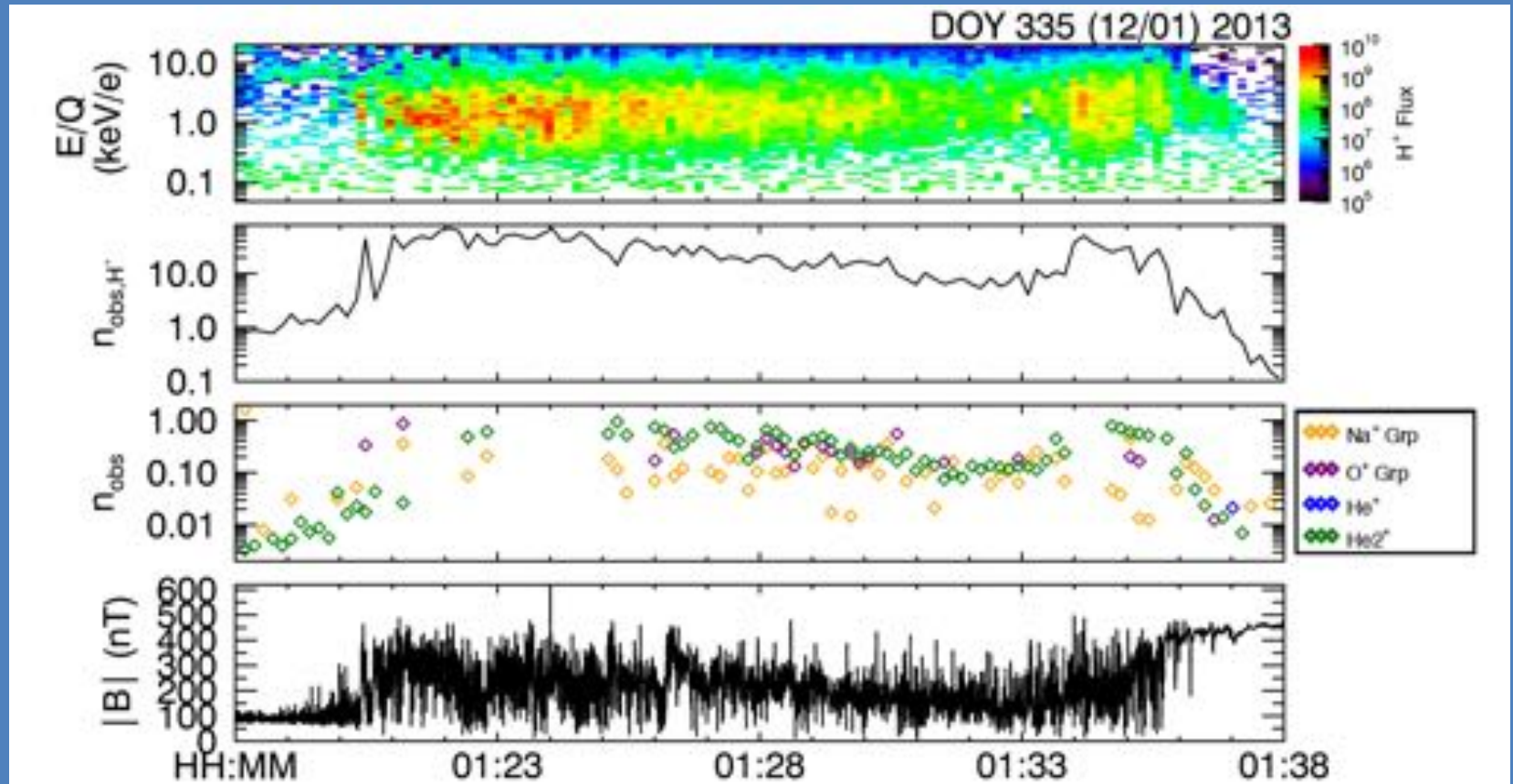
$P_{sw} \sim 140 \text{ nPa}$

DDM Magnetosheath



Slavin et al. (2018) $P_{\text{sw}} \sim 140 \text{ nPa}$

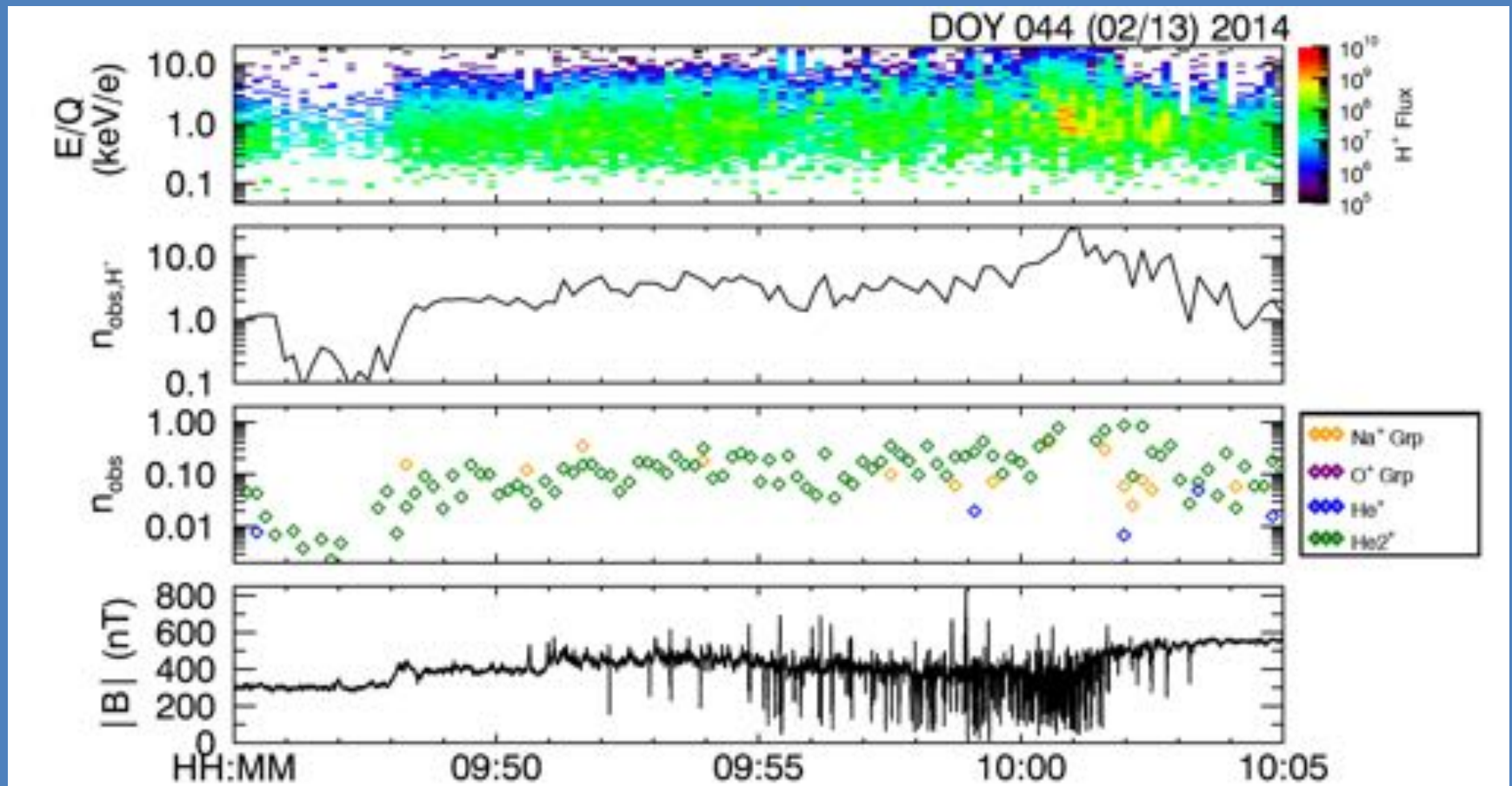
DDM Magnetosheath



$$P_{sw} \sim 180 \text{ nPa}$$

Slavin et al. (2018)

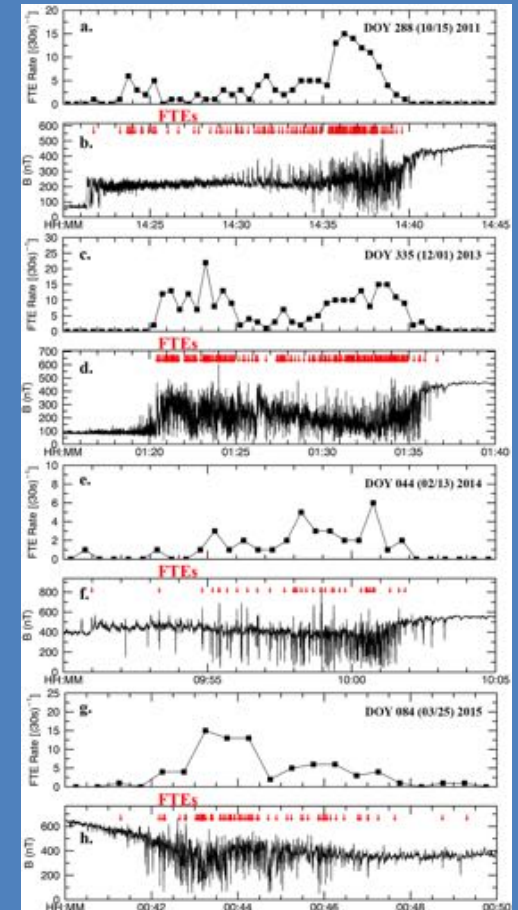
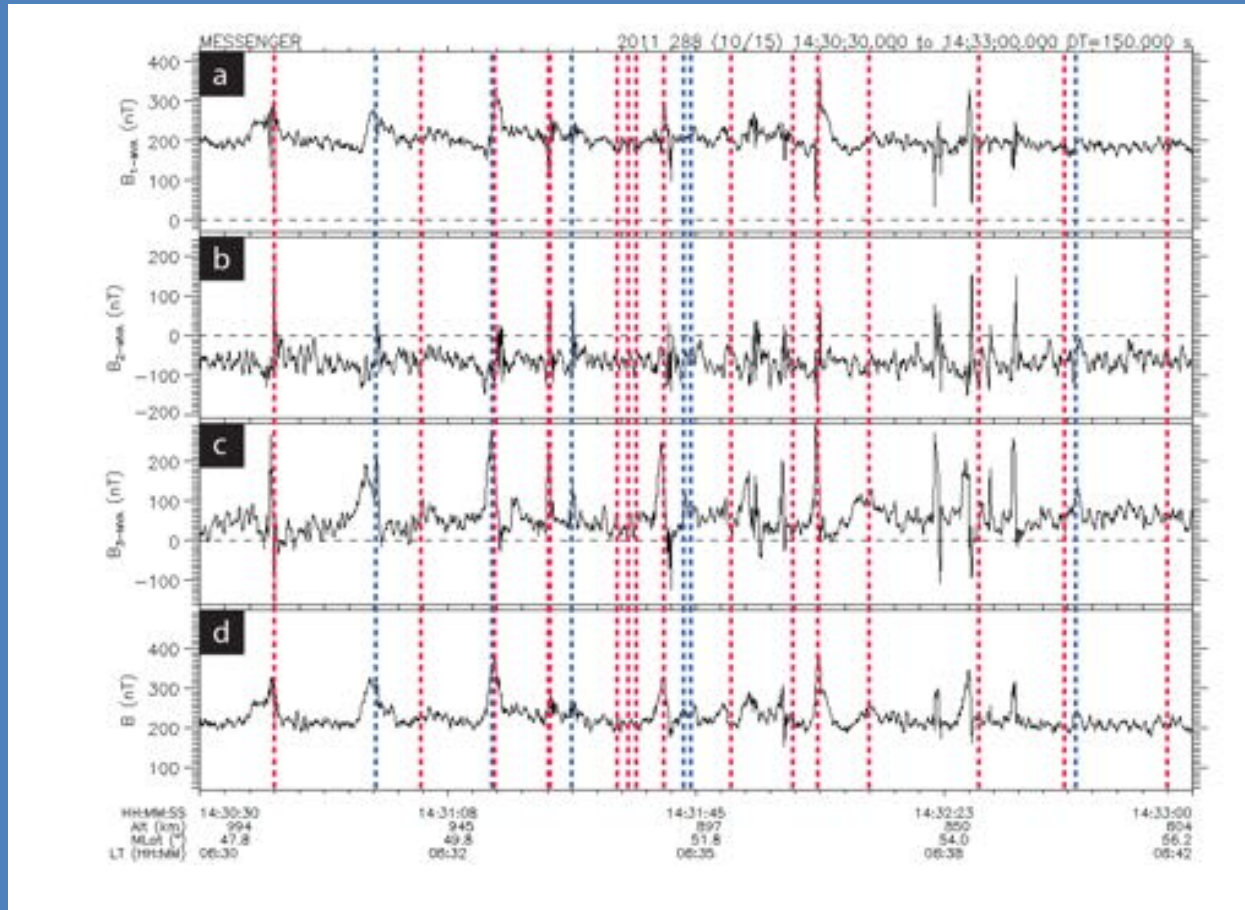
DDM Magnetosheath



$$P_{sw} \sim 290 \text{ nPa}$$

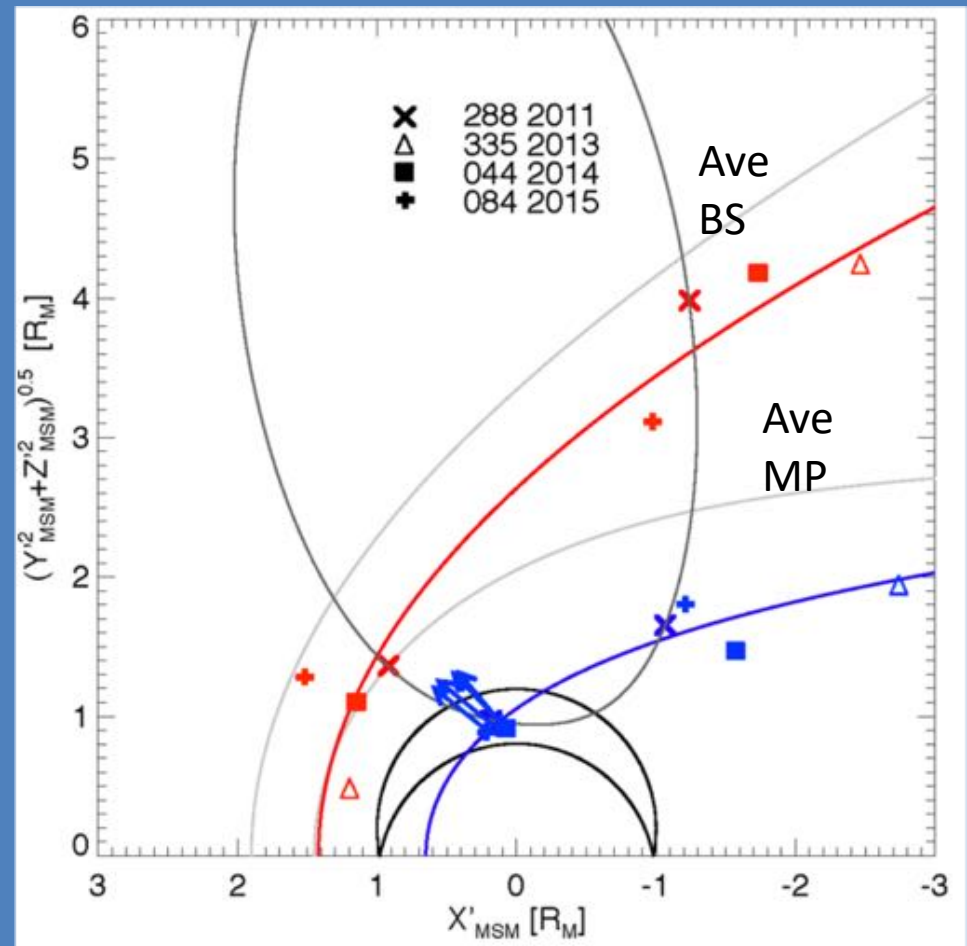
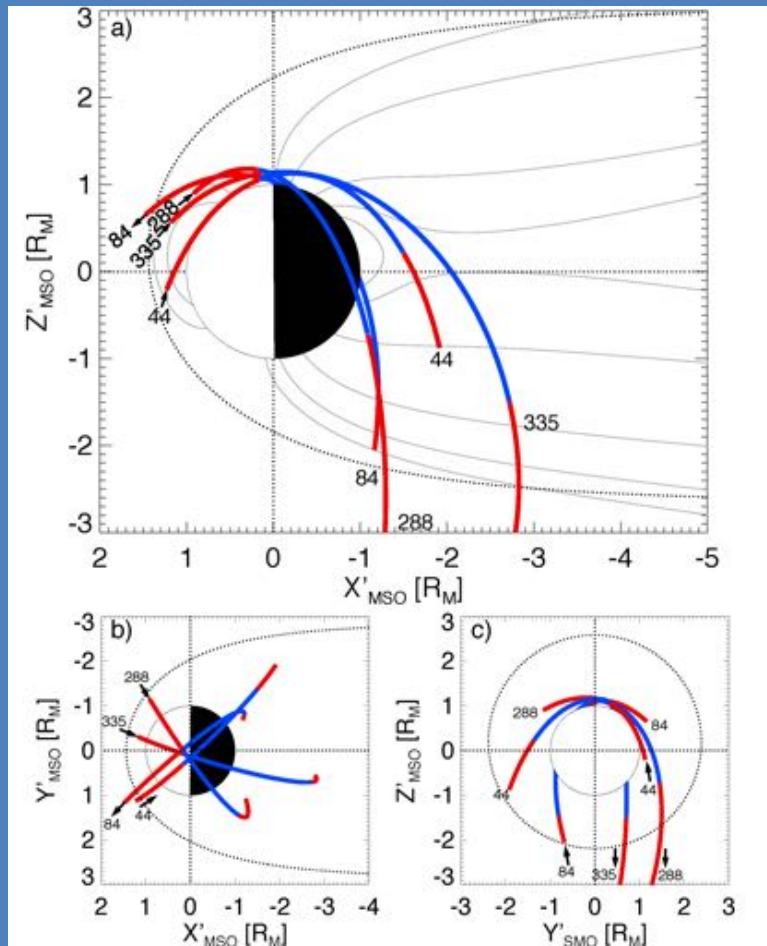
Slavin et al. (2018)

DDM Magnetosheath Flux Transfer Events



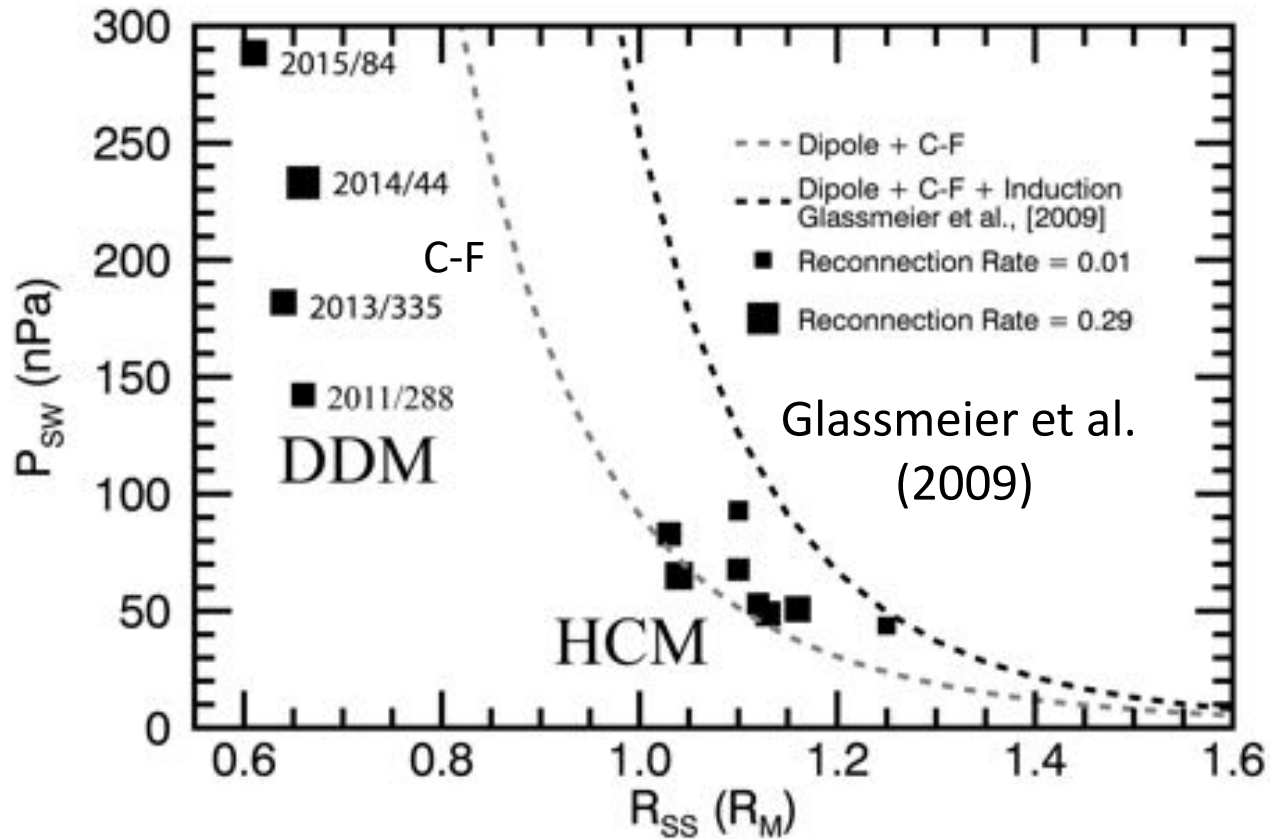
Slavin et al. (2018)

Low Altitude DDM Bow Shock & Magnetopause



Slavin et al. (2018)

Solar Wind Compression, Induction and Reconnection at Mercury



Slavin et al. (2018)

Summary

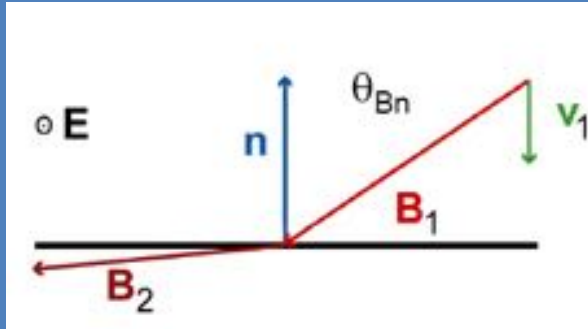
- Proximity to the Sun matters - - Mercury's magnetosheath tends to be low beta and develops a thick plasma depletion layer, which supports very fast symmetric reconnection. As a result reconnection driven dynamics at Mercury depends more upon IMF intensity and than southward IMF B_z (i.e. magnetic shear angle).
- Dimensionless reconnection rate at Mercury's magnetopause is ~ 3 to 10 times faster than at Earth) resulting in a "Dungey cycle" (i.e. substorm time cycle) of only ~ 3 min duration.
- Approximately once per Earth year MESSENGER observed "Disappearing Dayside Magnetosphere Events" that expose the forward hemisphere of Mercury's surface to direct solar wind impact. These DDMs appear due to CME associated extreme solar wind dynamics pressure and intense southward magnetosheath B_z .

Supplemental Material

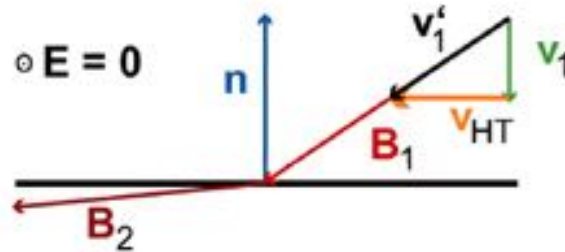
Shocks and Discontinuities

Two especially useful frames: the **normal incidence frame** and the **de-Hoffman-Teller frame**.

NIF



HTF



In the **normal incidence frame** the upstream flow is parallel to \mathbf{n} . There is a **motional electric field** $\mathbf{E}_u = -\mathbf{u}_u \times \mathbf{B}_u$, perpendicular to both \mathbf{u} and \mathbf{B} and parallel to the shock's plane.

To make **motional electric field zero**: to find a frame in which the upstream flow and magnetic field are parallel and the shock is stationary. This is obtained by adding a transformation velocity \mathbf{V}_{HT} parallel to the shock plane. New frame called **de Hoffman-Teller frame**.

Properties of HTF:

- ✧ Particles upstream have simple motion, parallel to magnetic field direction and gyration.
- ✧ Energy of a particle is constant
- ✧ Transformation velocity V_{HT} is the same downstream as it is upstream.

Conservation Laws

- In both fluid dynamics and MHD conservation equations for mass, energy and momentum have the form: $(\partial Q/\partial t) + \nabla \cdot \vec{F} = 0$, where Q and \vec{F} are the density and flux of the conserved quantity.
- If a discontinuity or shock is steady ($\partial/\partial t = 0$) and one-dimensional ($\partial F_n/\partial n = 1$ or $(\vec{F}_u - \vec{F}_d) \cdot \hat{n} = 0$, where u and d refer to upstream and downstream and \hat{n} is the unit normal to the discontinuity surface. We normally write this as a jump condition $[F_n] = 0$.
- Conservation of Mass $(\partial/\partial n)(\rho v_n) = 0$ or $[\rho v_n] = 0$.
- Conservation of Momentum $\rho v_n \frac{\partial v_n}{\partial n} + \frac{\partial p}{\partial n} + \frac{\partial}{\partial n} \left(\frac{B^2}{2\mu_0} \right) = 0$ where the first term is the rate of change of momentum and the second and third terms are the gradients of the gas and magnetic pressures in the normal direction.

$$\left[\rho v_n^2 + p + \left(B^2 / 2\mu_0 \right) \right] = 0$$

- Conservation of momentum: $[\rho v_n \vec{v}_t - (B_n / \mu_0) \vec{B}_t] = 0$
The subscript t refers to components that are transverse to the shock (i.e. parallel to the shock surface).
- Conservation of energy:

$$\left[\rho v_n \left(\frac{1}{2} v^2 + \frac{\gamma}{\gamma - 1} \frac{p}{\rho} \right) + v_n \frac{B^2}{\mu_0} - \vec{v} \cdot \vec{B} \frac{B_n}{\mu_0} \right] = 0$$

There we have used $p \rho^{-\gamma} = \text{const.}$ The first two terms are the flux of kinetic energy (flow energy and internal energy) while the last two terms come from the electromagnetic energy flux

- The jump conditions are a set of 6 equations. If we want to find the downstream quantities, given the upstream quantities, then there are 6 unknowns ($\rho, v_n, v_t, p, B_n, B_t$).
- The solutions to these equations are not necessarily shocks. These are conservation laws and a multitude of other discontinuities can also be described by these equations.

Types of Discontinuities in Ideal MHD		
Contact Discontinuity	$v_n = 0, B_n \neq 0$	Density jumps arbitrary, all others continuous. No plasma flow. Both sides flow together at v_t .
Tangential Discontinuity	$v_n = 0, B_n = 0$	Complete separation. Plasma pressure and field change arbitrarily, but pressure balance
Rotational Discontinuity	$v_n \neq 0, B_n \neq 0$ $v_n = B_n / (\mu_0 \rho)^{1/2}$	Large amplitude intermediate wave, field and flow change direction but not magnitude.

MHD Analysis Techniques

AOSS 595

Gang Kai Poh

Outline

- MHD Discontinuities
 - Tangential
 - Rotational
- Minimum Variance Analysis
- deHoffmann-Teller Frame Analysis
- Grad-Shafranov Reconstruction

MHD Discontinuities

- Rankine-Hugoniot Jump Conditions

$$\rho_{m,1} u_{n,1} = \rho_{m,2} u_{n,2}$$

$$\rho_{m,1} u_{n,1} \bar{u}_{t,1} - \frac{B_{n,1} \bar{B}_{t,1}}{\mu_0} = \rho_{m,2} u_{n,2} \bar{u}_{t,2} - \frac{B_{n,2} \bar{B}_{t,2}}{\mu_0}$$

$$\rho_m u_{n,1}^2 + p_1 + \frac{B_{t,1}^2 - B_{n,1}^2}{2\mu_0} = \rho_m u_{n,2}^2 + p_2 + \frac{B_{t,2}^2 - B_{n,2}^2}{2\mu_0}$$

$$u_{n,1} \bar{B}_{t,1} - B_{n,1} \bar{u}_{t,1} = u_{n,2} \bar{B}_{t,2} - B_{n,2} \bar{u}_{t,2}$$

$$B_{n,1} = B_{n,2}$$

$$\begin{aligned} & \frac{1}{2} \rho_m (u_{n,1}^2 + u_{t,1}^2) u_{n,1} + \frac{\gamma}{\gamma - 1} p u_{n,1} + \frac{B_{t,1}^2}{\mu_0} u_{n,1} - \frac{B_{n,1}}{\mu_0} (\bar{B}_{t,1} \cdot \bar{u}_{t,1}) \\ &= \frac{1}{2} \rho_m (u_{n,2}^2 + u_{t,2}^2) u_{n,2} + \frac{\gamma}{\gamma - 1} p u_{n,2} + \frac{B_{t,2}^2}{\mu_0} u_{n,2} - \frac{B_{n,2}}{\mu_0} (\bar{B}_{t,2} \cdot \bar{u}_{t,2}) \end{aligned}$$

Tangential Discontinuity

- Simplest case: $B_{n,1} = B_{n,2} = 0$
- Pressure Balance: $p_1 + \frac{B_{t,1}^2}{2\mu_0} = p_2 + \frac{B_{t,2}^2}{2\mu_0}$
- Plasma pressure, tangential B and density are discontinuous across discontinuity surface

Rotational Discontinuity

- Plasma pressure, tangential B and density are continuous across discontinuity surface
- $\rho_{m,1} = \rho_{m,2} \neq 0$, $u_{n,1} = u_{n,2} = u_n$ and $B_{n,1} = B_{n,2} = B_n$

$$\frac{\gamma}{\gamma - 1} p_1 + \frac{B_{t,1}^2}{\mu_0} = \frac{\gamma}{\gamma - 1} p_2 + \frac{B_{t,2}^2}{\mu_0}$$

Minimum Variance Analysis

An Overview

Minimum Variance Analysis

- Computation of the normal direction of the discontinuity to determine type of discontinuity
- Other applications include flux rope analysis
- Minimum Variance Analysis (MVA)
 - *Sonnerup and Cahill (1967)*
 - Analysis Methods for Multi-Spacecraft Data [*Sonnerup and Scheible, 1998*]
- Assumptions:
 1. Transitional layer is 1-D
 2. Time independent ($\frac{\partial}{\partial t} = 0$)
 3. Minimum set of 3 vectors required

Minimum Variance Analysis

- Method is used to determine the B-field in the normal direction \hat{n} [Sonnerup and Scheible, 1998]
- \hat{n} is defined as minimum variance direction (i.e. direction in which B-field varies the least)
 - Can be expressed in the following equation:

$$\min \sigma^2 = \min \frac{1}{M} \sum_{m=1}^M |(\bar{B}^{(m)} - \langle \bar{B} \rangle) \cdot \hat{n}|^2$$

- Solution can be written as a eigenvalue-eigenvector problem:

$$\sum_{\nu=1}^3 M_{\mu\nu}^B n_{\nu} = \lambda n_{\mu}$$

$$M_{\mu\nu}^B = \langle B_{\mu} B_{\nu} \rangle - \langle B_{\mu} \rangle \langle B_{\nu} \rangle$$

- Results are 3 eigenvectors that forms an orthogonal basis and corresponding 3 eigenvalues
- The eigenvector that corresponds to smallest eigenvalue is defined as \hat{n}

APPROVED FOR THE
FAINT-HEARTED!!

Recipe for MVA

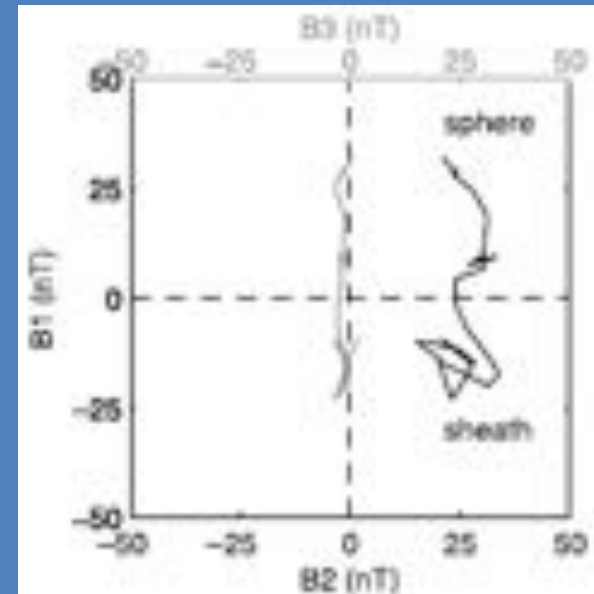
- Step 1: Construct the covariance matrix $M_{\mu\nu}$ (See previous slide)
- Step 2: Solve the eigen-problem by diagonalizing $M_{\mu\nu}$
 - Express $M_{\mu\nu} = PDP^{-1}$, where P is an invertible matrix and D is the diagonal matrix
 - Each columns of matrix P corresponds to each eigenvectors that form the basis for the MVA coordinate system.
 - Each diagonal term of D corresponds to the individual eigenvalues
 - Computation of eigen-values/vectors is non-trivial (even for 3x3 matrix), hence numerical methods using preferred programming language is recommended (e.g. Matlab, IDL or Mathematica etc)

Recipe for MVA

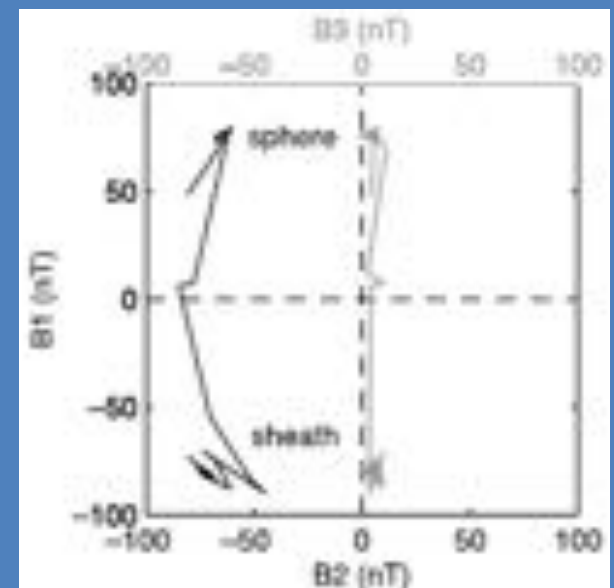
- Step 3: Transformation of magnetic field data in xyz coordinate (or any other coordinate system) into the MVA coordinate system using the eigenvectors computed from Step 2.
 - Example: We have a set of N numbers of data points for B_x , B_y and B_z
 - After performing MVA on the data set, we obtained 3 eigenvectors: \bar{x}_{min} , \bar{x}_{int} , \bar{x}_{max} that form the basis for the MVA coordinate system.
 - We can then find the vector in MVA coordinate by doing dot product for each xyz magnetic field vector on each eigenvector (i.e. coordinate transformation)
 - E.g. $\bar{B} \cdot \bar{x}_{min} = B_{min}$

Examples:

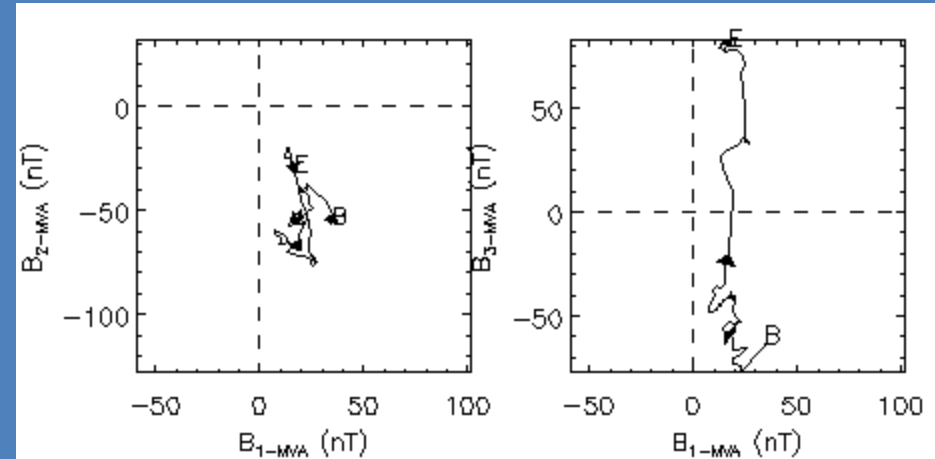
- Normal direction $\hat{x}_3 = (0.88, 0.46, -0.14)$
- Little deviation from $\langle B_3 \rangle = 0$ for B_1 - B_3 hodogram suggest tangential discontinuity
- Unclear signature for B_1 - B_3 hodogram also suggest rotational discontinuity



- Normal direction $\hat{x}_3 = (-0.98, 0.04, 0.17)$
- Little deviation from $\langle B_3 \rangle \neq 0$ for B_1 - B_3 hodogram and clear rotational signature for B_1 - B_3 hodogram strongly suggest rotational discontinuity



Better Examples (MESSENGER)



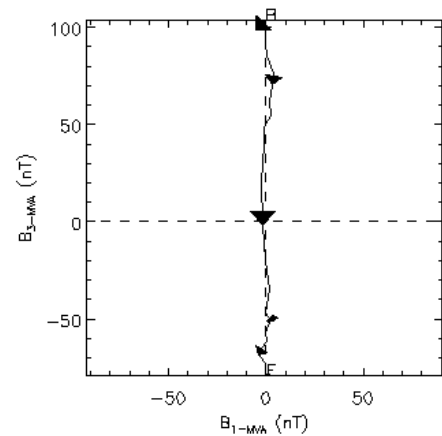
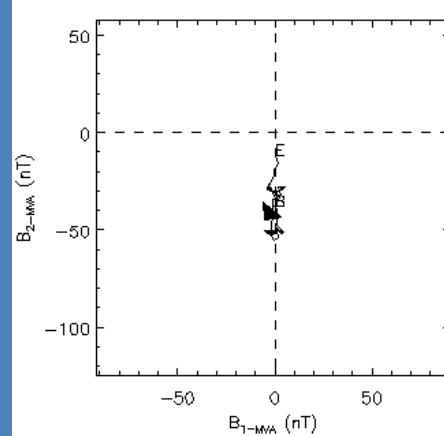
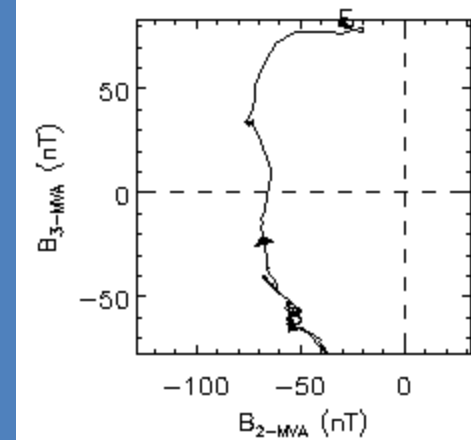
Minimum Variance Analysis
 $e_{21}=6.90$
 $e_{33}=14.11$
 Number of points=107 Nsmooth=0

1-MIN 2-INTERMEDIATE 3-MAX VARIANCE DIRECTION

	1	2	3
X	-0.305	-0.944	0.129
Y	0.745	-0.152	0.650
Z	-0.594	0.295	0.749
EVAL	27.593	190.042	2680.776

ANGLE MIN VAR DIRECTION and B: $72.3 \pm 4.61^\circ$
 ANGLE MAX VAR DIRECTION and B: $74.2 \pm 4.03^\circ$
 $\langle B_{\text{ave}} \rangle = 87.8, 85.7$ nT SHEAR ANGLE=12.5
 $\langle B1 \rangle = 18.76 \pm 2.49$ nT
 $\langle B2 \rangle = -56.23$ nT
 $\langle B3 \rangle = -18.80$ nT

ROTATION ANGLE (CENTROID) = -3.39 radians
 AVE. FREQUENCY (CENTROID) = -0.1001 Hz
 ESTIMATED ELLIPTICITY = -0.247 ± 0.00524
 MVA Normal -0.305 0.745 -0.594 rad
 Tan.Dis. Normal 0.586 -0.662 0.466 rad
 ANGLE between normals: 18.367 DEGREES
 Sines Normal -0.305 0.745 -0.594 rad
 ANGLE between normals: NaN DEGREES



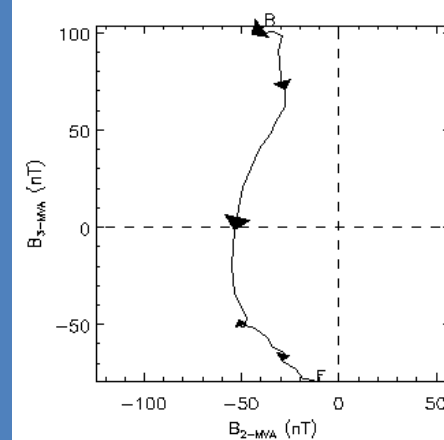
Minimum Variance Analysis
 $e_{21}=29.82$
 $e_{32}=32.73$
 Number of points=30 Nsmooth=0

1-MIN 2-INTERMEDIATE 3-MAX VARIANCE DIRECTION

	1	2	3
X	0.889	0.439	-0.130
Y	-0.353	0.837	0.418
Z	0.292	-0.326	0.899
EVAL	4.565	136.146	4456.861

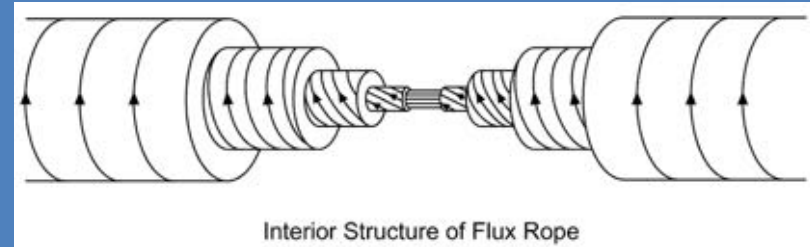
ANGLE MIN VAR DIRECTION and B: $89.4 \pm 7.10^\circ$
 ANGLE MAX VAR DIRECTION and B: $88.2 \pm 6.43^\circ$
 $\langle B_{\text{ave}} \rangle = 108., 80.0$ nT SHEAR ANGLE=14.8
 $\langle B1 \rangle = 0.40 \pm 1.35$ nT
 $\langle B2 \rangle = -36.61$ nT
 $\langle B3 \rangle = 1.13$ nT

ROTATION ANGLE (CENTROID) = 3.43 radians
 AVE. FREQUENCY (CENTROID) = 0.3617 Hz
 ESTIMATED ELLIPTICITY = 0.172 ± 0.00209
 MVA Normal 0.889 0.439 -0.353 0.292
 Tan.Dis. Normal -0.894 0.343 -0.288
 ANGLE between normals: 0.631 DEGREES



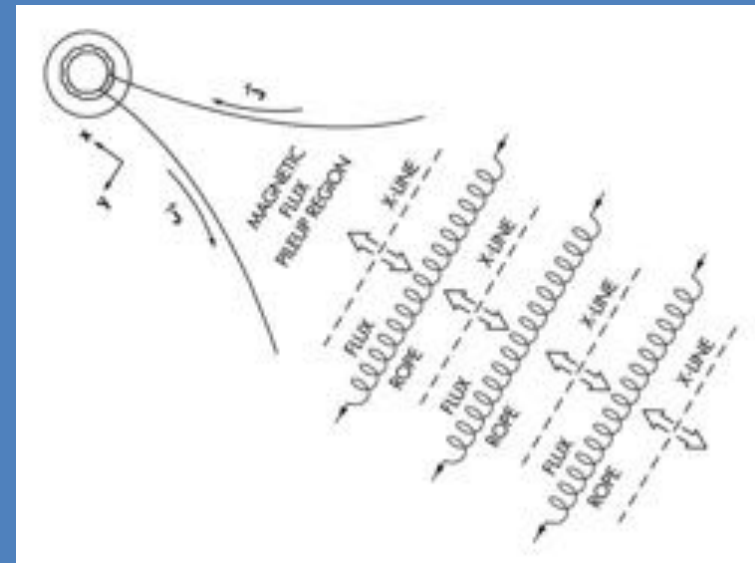
Flux Ropes

- What is a Flux Rope?
 - Helical magnetic flux tube with a strong core field
 - Common phenomenon in space plasma physics
- Formation of FR at planetary magnetospheres
 - Flux Transfer Events (FTEs) at magnetopause are flux ropes too
 - Widely-accepted formation theory is multiple X-line reconnection at the plasma sheet in the magnetotail
 - FR formed at the magnetotail can be classified into 2 categories [Slavin et al 2003a,b]:
 - Earthward propagating Bursty Bulk Flow (BBF)
 - Tailward propagating plasmoid



Interior Structure of Flux Rope

Russell and Elphic, 1979



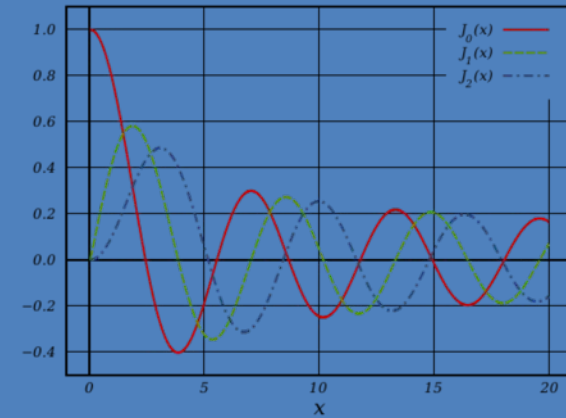
Slavin et al., 2002

Common Flux rope Analysis Technique

- Force-Free Flux Rope Model
 - *Burlaga [1988], Lepping et al., [1990]*

- Assumptions:
 1. Force free ($\vec{J} \times \vec{B} = 0$)
 2. Cylindrical geometry

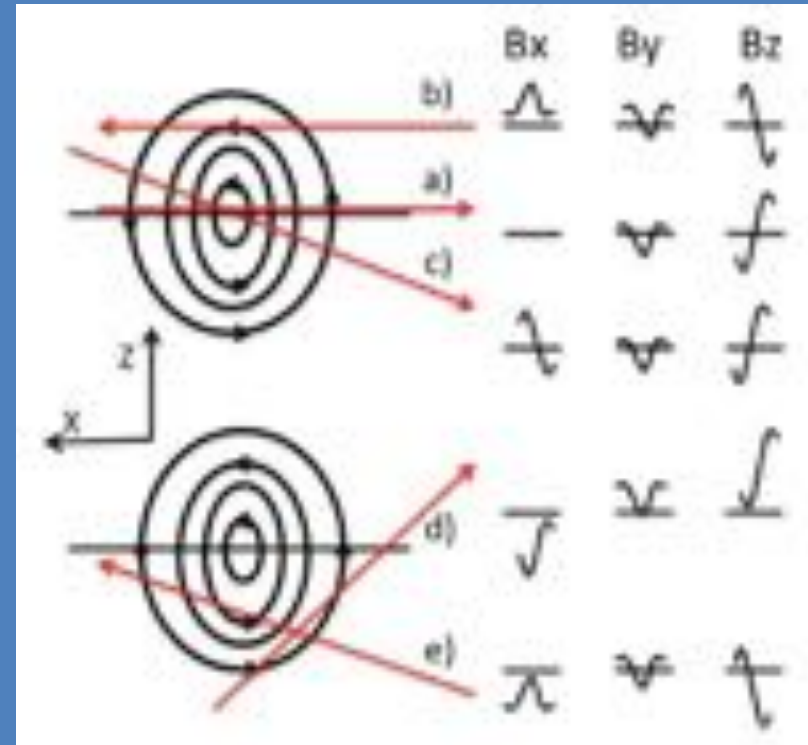
$$\begin{array}{l} \text{Axial Component} \\ B_A = B_0 J_0(\alpha R) \\ \\ \text{Tangential Component} \\ B_T = B_0 H J_1(\alpha R) \end{array}$$



- Force-free equation ($\nabla \times \vec{B} = \alpha \vec{B}$) can be solve analytically in cylindrical coordinate [*Lundquist, 1950*]
- Model results is fitted to data to infer physical properties of flux rope
- Limitations:
 1. Flux ropes are rarely force free due to internal/external plasma pressure acting on the structure
 2. Only 60% of the flux ropes agrees reasonably well with the force-free model while the remaining 40% cannot be modeled Slavin et al., 2003b

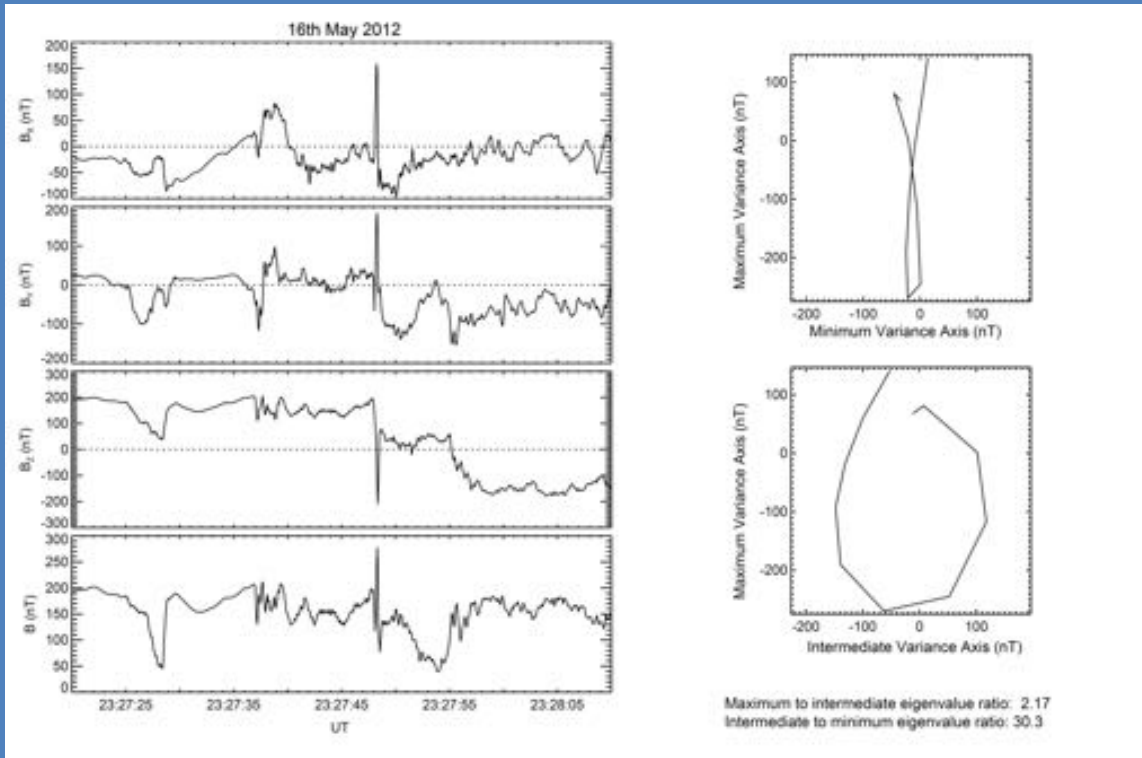
MVA Flux Rope Analysis

- MVA is common tool used to analyze Flux Ropes everywhere
- MVA can be used to determine the direction of 3 axis of the helical structure.
- In an ideal situation (as shown from figure above)
 - Minimum direction is parallel to direction of travel
 - Intermediate direction is parallel to the axis of the flux rope
 - Maximum direction is in the direction of the rotation of the field.
- Limitations?



Borg et al., 2012

Example of MVA on Flux Rope Analysis



- Notice that the eigen value ratios are > 1.5 . Typically eigenvalue ratio > 1.5 suggest that the eigenvectors are well determined.
- If eigenvalues ratios < 1.5 , the eigenvalues are degenerate, which means the corresponding eigenvectors are not unique.
- This could also suggest that the magnetic structure is 2-D in nature.
- Examples: Travelling Compression Regions (TCRs)

deHoffmann-Teller Analysis An Overview

deHoffmann-Teller (HT) Analysis

- Convection electric field $\bar{E} = -\bar{v} \times \bar{B}$ in the observer frame of reference
- HT frame is the frame of reference where \bar{E} vanishes
- To determine properties of the MHD structure, it is important to determine the HT frame velocity
- For simplicity, we will discuss the HT frame analysis for 1-D structures such as shocks and MHD discontinuities

deHoffmann-Teller Frame

- Frozen-in condition requires presence of convection E-field ($\vec{E} = -\vec{v} \times \vec{B}$) in observer frame
- Transforming into a frame where $\vec{E} \sim 0$
 - This frame is known as the deHoffmann-Teller (HT) Frame [*deHoffmann and Teller, 1950*]
 - Non-iterative, least-square method first developed by *Sonnerup et al [1987, 1990]* to determine the HT velocity \vec{v}_{HT}

• Theory:

- Define the mean square of the electric field $D(v)$ to be:

$$D(v) = \frac{1}{M} \sum_{i=1}^M |E'^{(i)}|^2 = \frac{1}{M} \sum_{i=1}^M |(v^{(i)} - V) \times B^{(i)}|^2$$

- V is the HT velocity that minimize $D(v)$ (i.e. $\nabla_V D(v) = 0$)
- Solution is given by:

- Equation above can be rearrange to become: $K_0 V_{HT} = \langle K^{(i)} v^{(i)} \rangle$

$$V_{HT} = K_0^{-1} \langle K^{(i)} v^{(i)} \rangle$$

deHoffmann-Teller Frame

- $K^{(i)}$ is defined as the projection matrix onto the plane perpendicular to $B^{(i)}$ multiplied by $B^{(m)2}$ and is given by the equation:

$$K_{\nu\mu}^{(i)} = B^{(i)2} \left(\delta_{\nu\mu} - \frac{B_{\mu}^{(i)} B_{\nu}^{(i)}}{B^{(m)2}} \right)$$

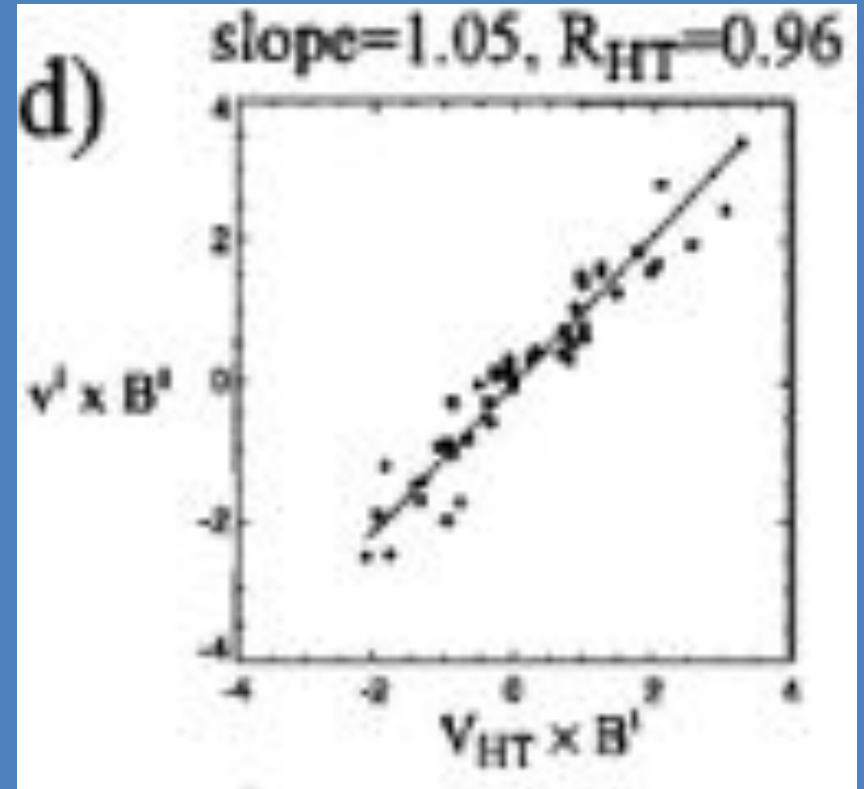
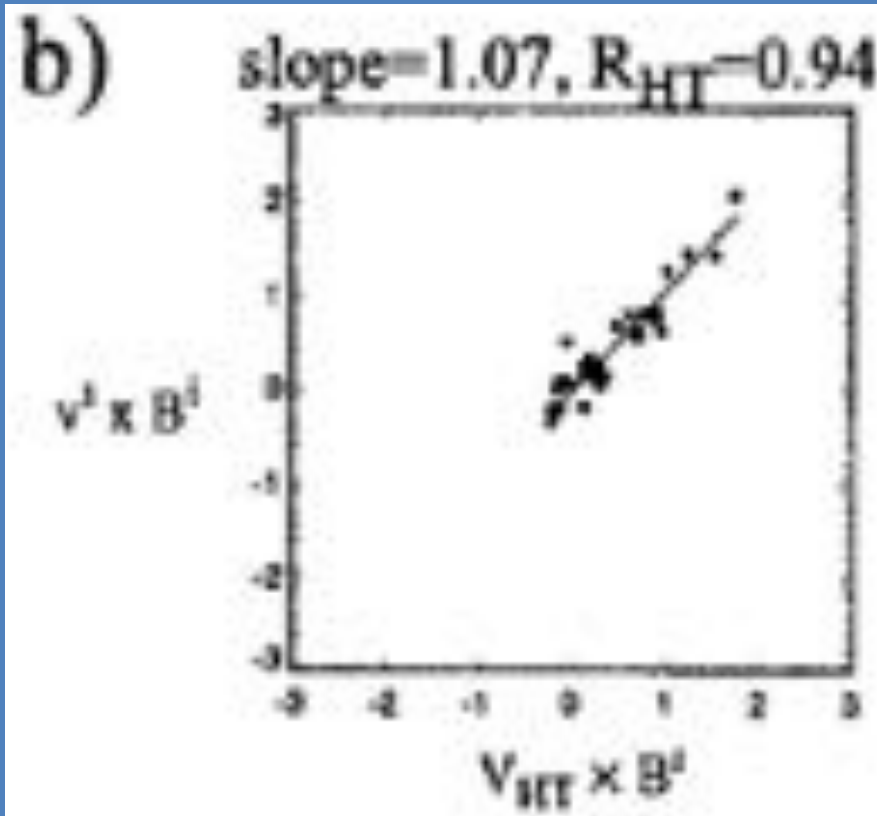
- K_0 is then defined as:

$$K_0 \equiv \langle K^{(i)} \rangle$$

deHoffmann-Teller (HT) Analysis

- Determine quality of HT frame
- Correlation comparison between:
 - Convection ($\bar{E}_c^{(i)} = -\bar{v}^{(i)} \times \bar{B}^{(i)}$) E-field
 - HT ($\bar{E}_{HT}^{(i)} = -\bar{V}_{HT} \times \bar{B}^{(i)}$) E-field
- High correlation means well-determined HT frame and vice versa
- One of the reasons for poorly-determined HT frame could be due to acceleration of the frame
- Hence, the acceleration term had to be accounted for before the HT velocity could be used for further analysis

Example:



Walén Condition

- For a rotational discontinuity, accelerated plasma flow is alfvénic in the HT frame
- Walén Relation

$$v' = v - V_{HT} = \pm \frac{\bar{B}}{\sqrt{\mu_0 \rho}}$$

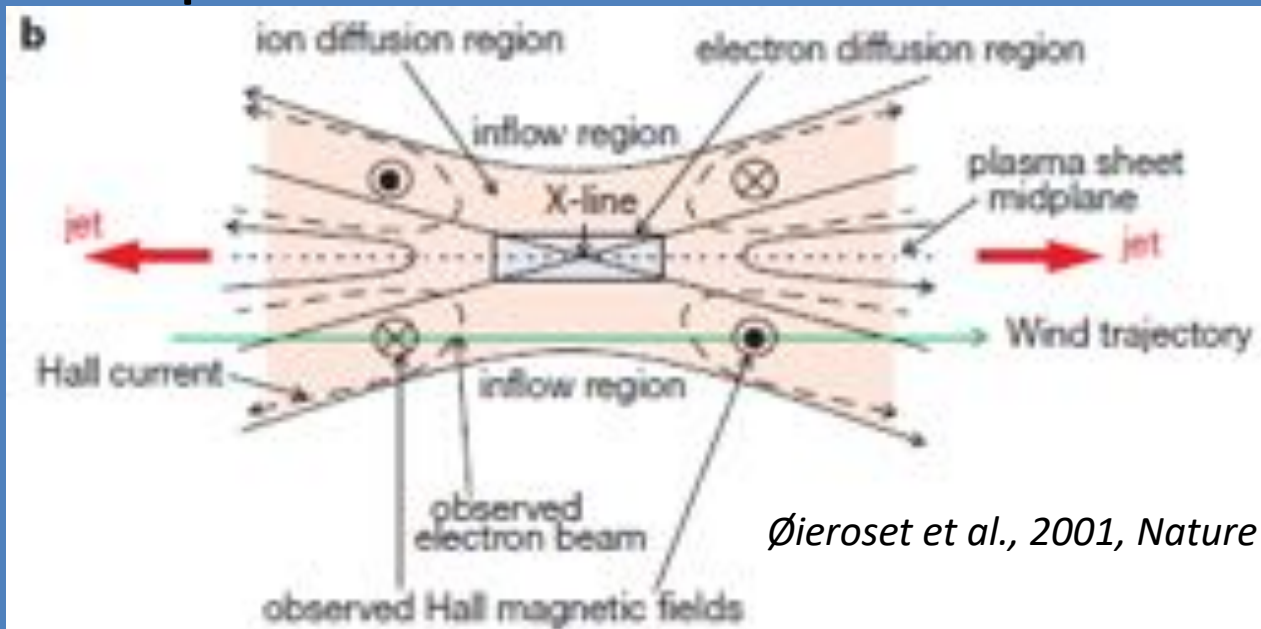
- This relation has major application in understanding magnetic reconnection

Magnetic Reconnection

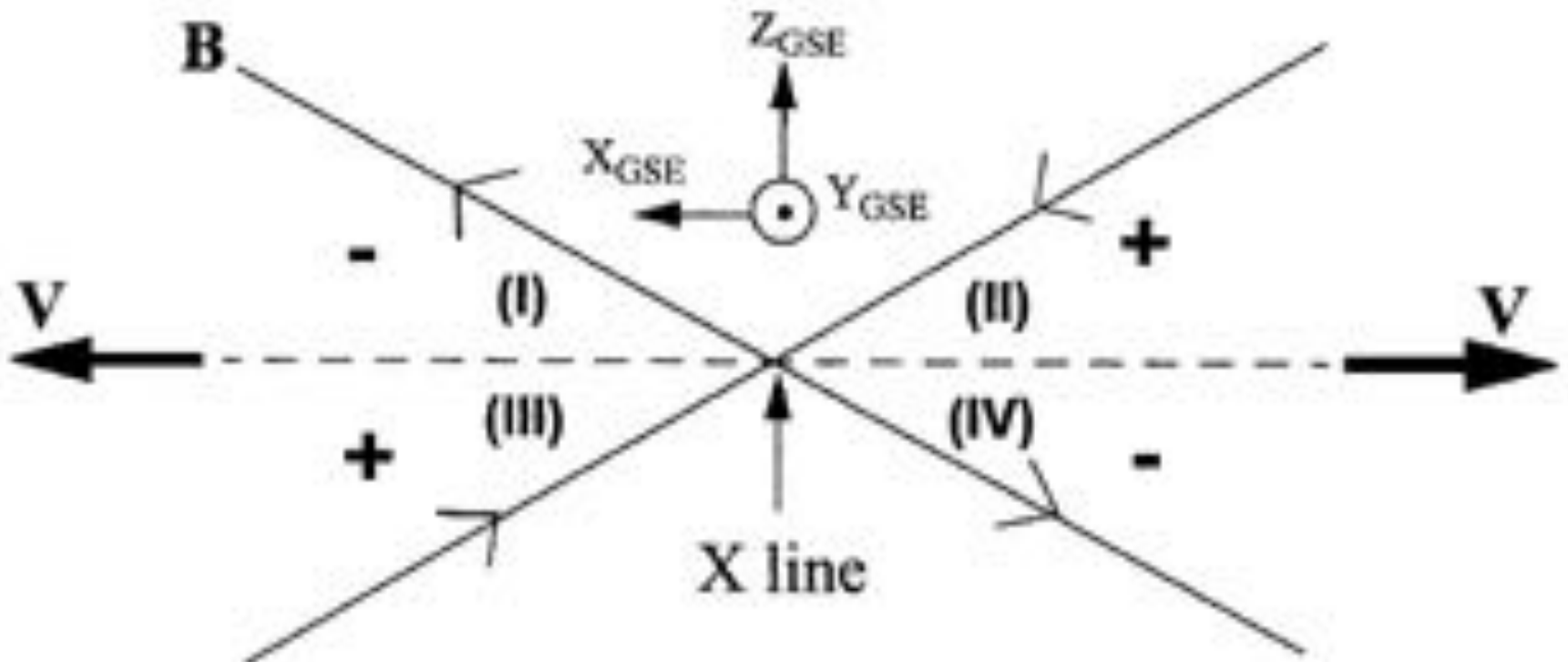
- Generalized Ohm's Law

$$\mathbf{E} + \mathbf{v} \times \mathbf{B} = \eta \mathbf{J} + \frac{1}{ne} \mathbf{J} \times \mathbf{B} - \frac{1}{ne} \nabla P + \frac{m_e}{ne^2} \frac{\partial \mathbf{J}}{\partial t}$$

- De-magnetization of protons results in quadrupolar Hall field in the diffusion region



Magnetic Reconnection

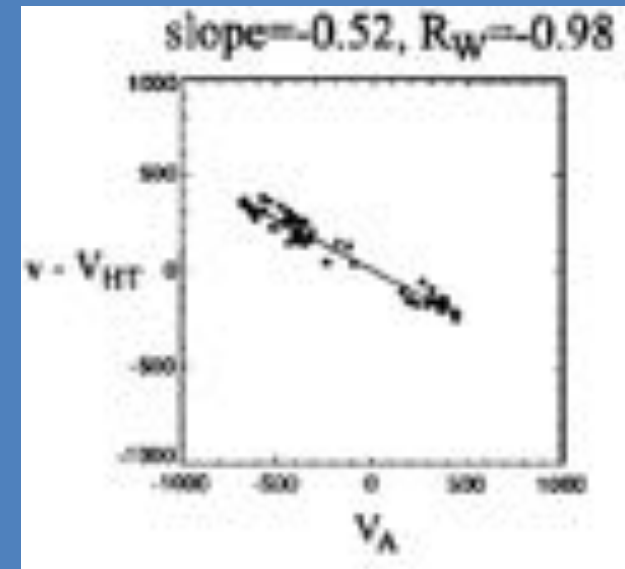
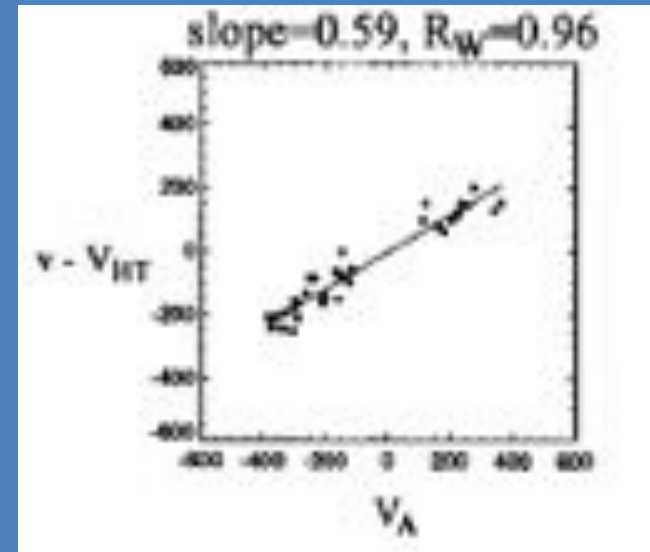


Walén Condition Example:

- (Upper) Good correlation between flow velocity in HT frame and local Alfvén velocity.
- Positive correlation suggest flow in region I/III of quadrupolar field
- Flow is only 59% of V_A

Øieroset et al., 2000, JGR

- (Lower) Again, good correlation between flow velocity in HT frame and local Alfvén velocity.
- Negative correlation suggest flow in region II/IV of quadrupolar field
- Flow is only 52% of V_A



Grad-Shafranov Reconstruction

An Overview

Some Definitions

- Reconstruction plane is the xy -plane
- Invariant axis z means $\frac{\partial}{\partial z} = 0$
- Transverse means the x, y components
- Magnetic potential vector \bar{A} in the \hat{z}
 - $\bar{B} = \nabla \times \bar{A}$
 - $A(x,y)$ is the stream function for the field lines

Assumptions

- Magnetic structure is approx. 2-D
- Proper frame where the structure appears stationary i.e. $\frac{\partial}{\partial t} = 0$
 - The deHoffmann-Teller frame
- Convective inertia term neglected in the momentum equation
- Transverse Pressure, B_z and thermal pressure are field line invariants
 - Only dependent on magnetic potential A

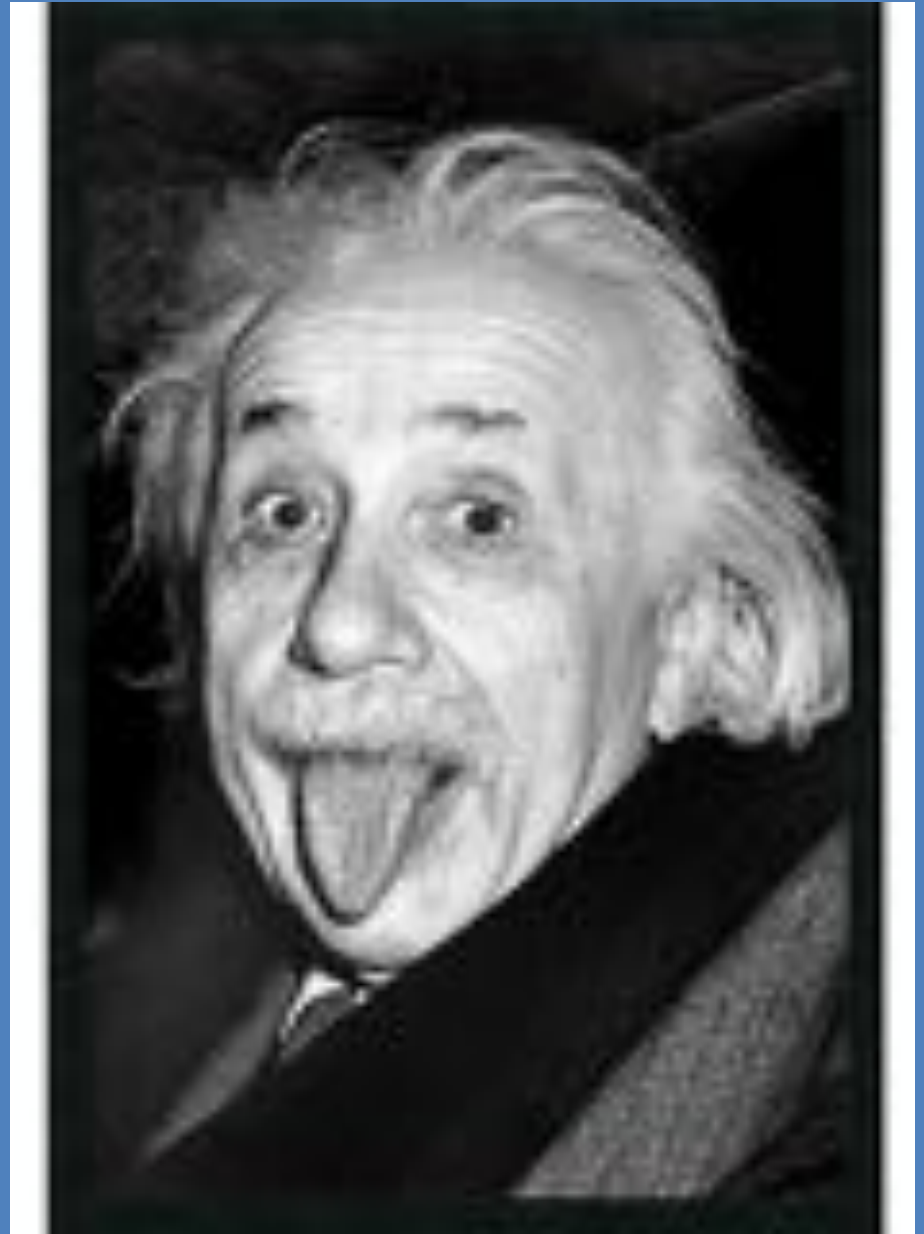
Grad-Shafranov Equation

- For a 2-D, coherent, magnetohydrostatic structure

$$\nabla_t p = \bar{J} \times \bar{B}$$

- After some math and

Become like this!!



Grad-Shafranov Equation

- You get the Grad-Shafranov Equation

$$\nabla^2 A = \frac{\partial^2 A}{\partial x^2} + \frac{\partial^2 A}{\partial y^2} = -\mu_0 \frac{d}{dA} \left(p + \frac{B_z^2}{2\mu_0} \right)$$

The Recipe

- Reconstruction process uses the GSE components of:
 - B-field
 - plasma velocity
 - plasma density
 - Temperature
- Step 1: Use minimum-variance analysis (MVA) to find the normal vector \hat{n} (Sonnerup and Scheible[1998])
- Step 2: Determine the HT frame velocity \bar{V}_{HT} and construct the Walen plot to justify the neglecting of inertia terms (Khrabrov and Sonnerup[1998])

How to determine if a good frame is chosen?

$$E^{(m)} = -v^{(m)} \times B^{(m)}$$

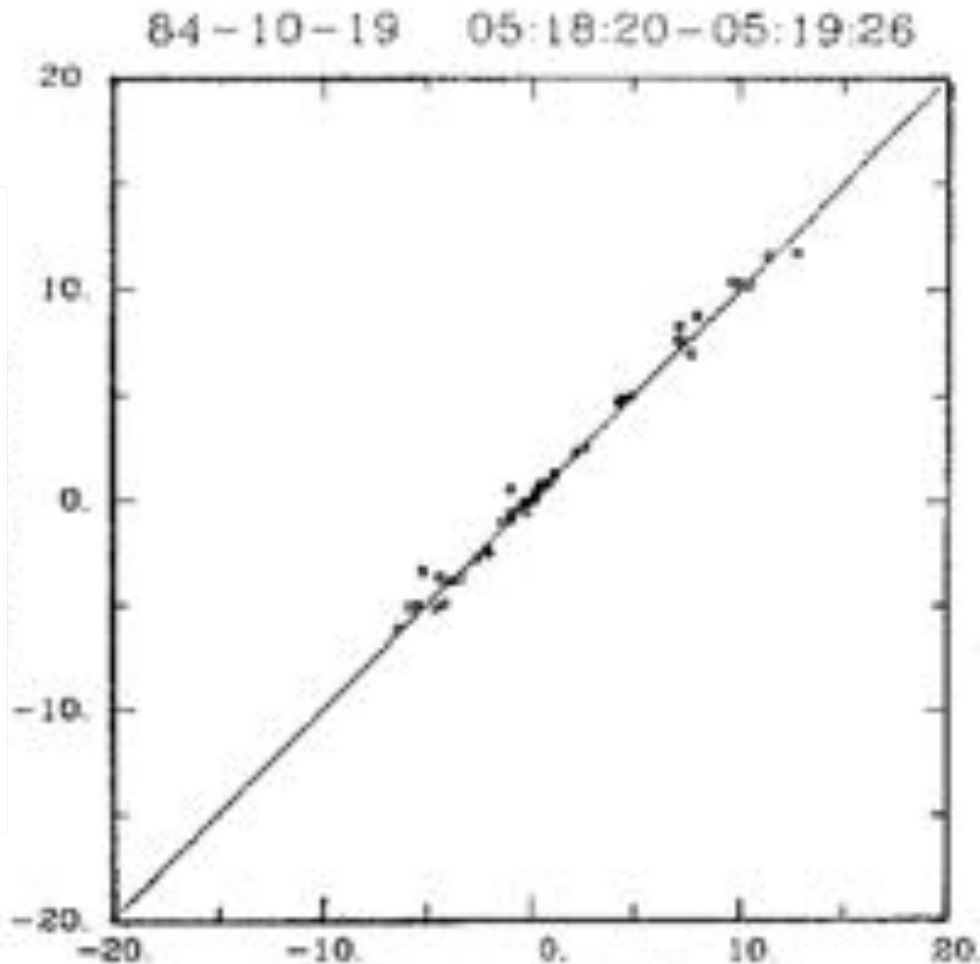


Figure from
Khrabrov & Sonnerup 1998

$$E_{HT}^{(m)} = -v_{HT} \times B^{(m)}$$

What is a Walen plot?

- Basically it is a component-by-component scatterplot of plasma velocities in the HT frame and their relation to the local measured

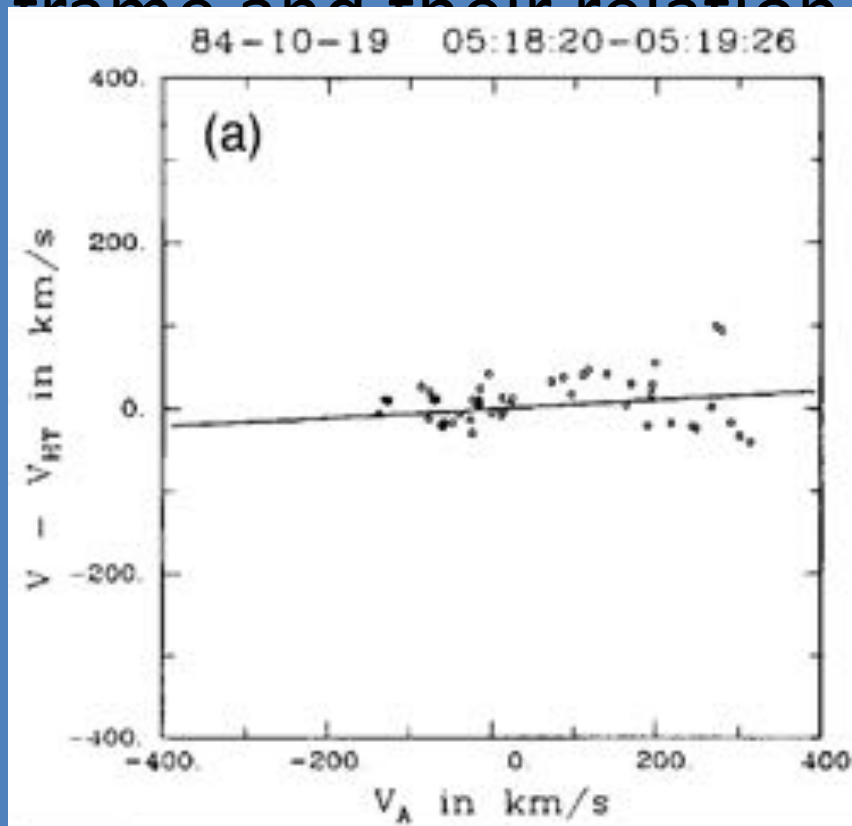


Figure from
Khrabrov & Sonnerup 1998

The Recipe

- Step 3: Select the invariant axis $\hat{\hat{z}}$ and the corresponding unit vector $\hat{\hat{x}}$ and $\hat{\hat{y}}$
- Step 4: Projection of HT velocity \bar{V}_{HT} onto the $\tilde{x}\tilde{y}$ plane to obtain \bar{V}_{HTi}
 - let the unit vector \hat{x} to lie along $-\bar{V}_{HTi}$
 - $\hat{z} = \hat{\hat{z}}$
 - $\hat{y} = \hat{z} \times \hat{x}$
- Step 5: Interpolation of data using a cubic spline

The Recipe

- Step 6: Obtain $A(x,0)$ along the spacecraft trajectory by integrating $B_y = -\frac{\partial A}{\partial x}$

$$A(x,0) = -\int B_y dx \quad , \quad A(x,0) = -V_0 \int_0^{t'} B_y dt'$$

- Step 7: Function of $P + \frac{B_z^2}{2\mu_0}$ w.r.t $A(x,0)$ can be prepared and differentiated for use on the R.H.S of the GS equation
 - Flux ropes: Single-value function
 - Magnetopause: Possibly double-value function

The Recipe

- Step 8: Treating it as a spatial initial problem, we can then Taylor expand $A(x, \pm\Delta y)$ into:

$$A(x, \pm\Delta y) = A(x, 0) \pm (\Delta y) \frac{dA(x, 0)}{dy} + (\Delta y)^2 \frac{d^2A}{dy^2} + \dots$$

$$A(x, \pm\Delta y) = A(x, 0) + (\Delta y)B_x(x, 0) + (\Delta y)^2 \frac{d^2A}{dy^2}$$

– With $\frac{d^2A}{dy^2} = -\frac{d^2A}{dx^2} - \mu_0 \frac{dP_t}{dA}$

- A new value of B_x can be computed by Taylor expanding B_x :

$$B_x(x, \pm\Delta y) = B_x(x, 0) \pm (\Delta y) \frac{dB_x}{dy} = B_x(x, 0) \pm (\Delta y) \frac{d^2A(x, 0)}{dy^2}$$

The Recipe

- Step 9: Finite Difference Method to evaluate

$$\left(\frac{d^2 A}{dx^2}\right)_i = \frac{2A_i - 5A_{i+1} + 4A_{i+2} - 2A_{i+3}}{(\Delta x)^2}$$

Central Difference

- Integration domain is rectangular, as compared to rhombus shaped

The Recipe

- Solving the GS equation as an initial value problem (Cauchy Problem) leads to numerical instability
 - Exponential growth
- Need for a “suppressing” algorithm
 - Do a running, 3-point, weighted averages
- To extend the integration domain, a total pressure adjustment method is introduced (Hu and Sonnerup 2003)

Why GS Reconstruction?

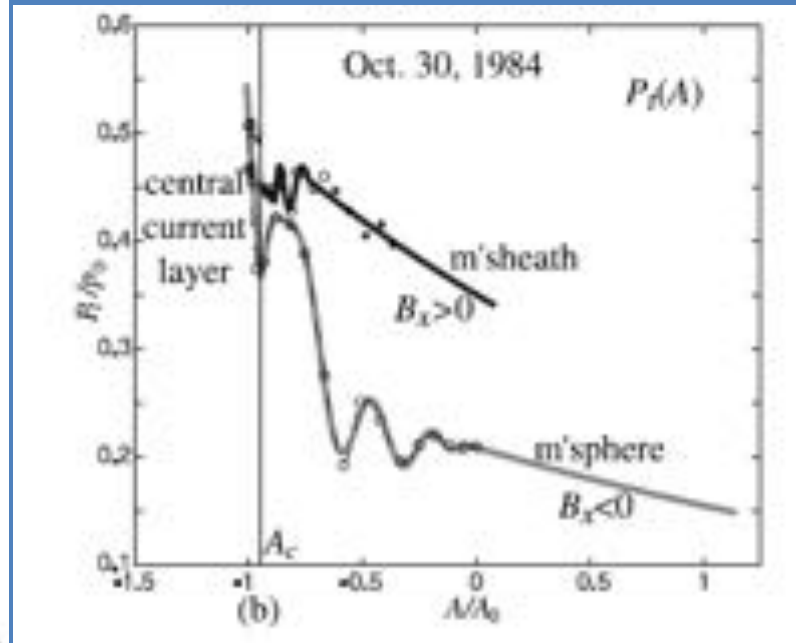
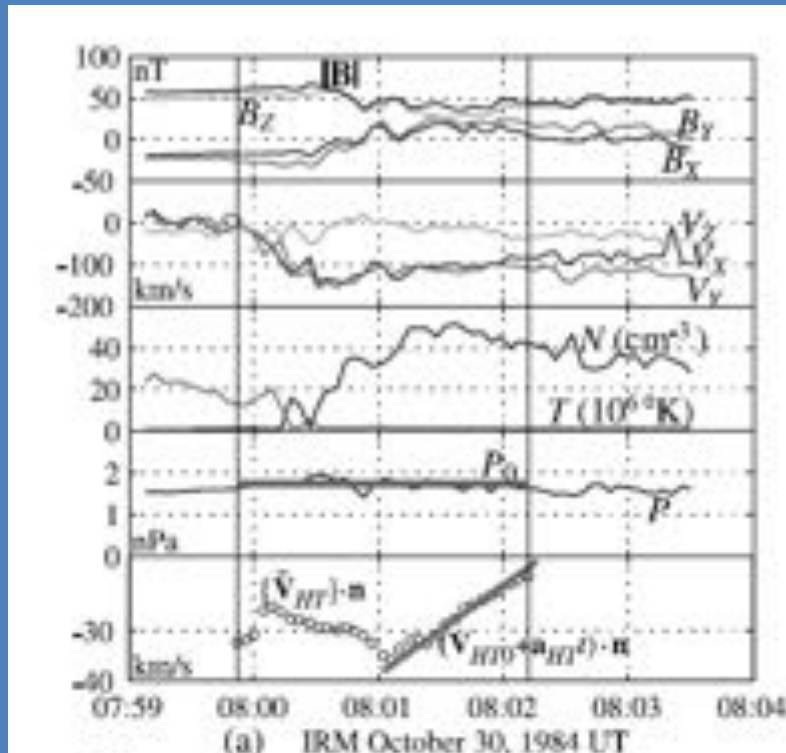
- Common method to determine physical and magnetic properties of flux ropes: Fitting of a Bessel Function solution to the force-free equation
 - Makes assumption of its structure such as axisymmetric
 - GS Reconstruction doesn't
- Magnetic Structures of the magnetopause
 - X-Type nulls
 - Presence of magnetic islands
- Besides the fact that it also creates 2.5/3 dimensional pretty plots!!!
 - Magnetic transects

What can we learn through GS-Reconstruction?

Magnetic Properties	Physical Properties
Maximum axial field strength	Velocity and direction in which the structure is travelling (whether it is accelerating, decelerating or constant velocity)
Magnetic topology	Size/diameter
Helicity	Axis orientation
Plasma Properties such as axial current, plasma pressure, number density and temperature	Twist of field lines
Chirality	Impact parameters
Presence of magnetic island and X-lines	Expansion or contraction
	Position of X-lines

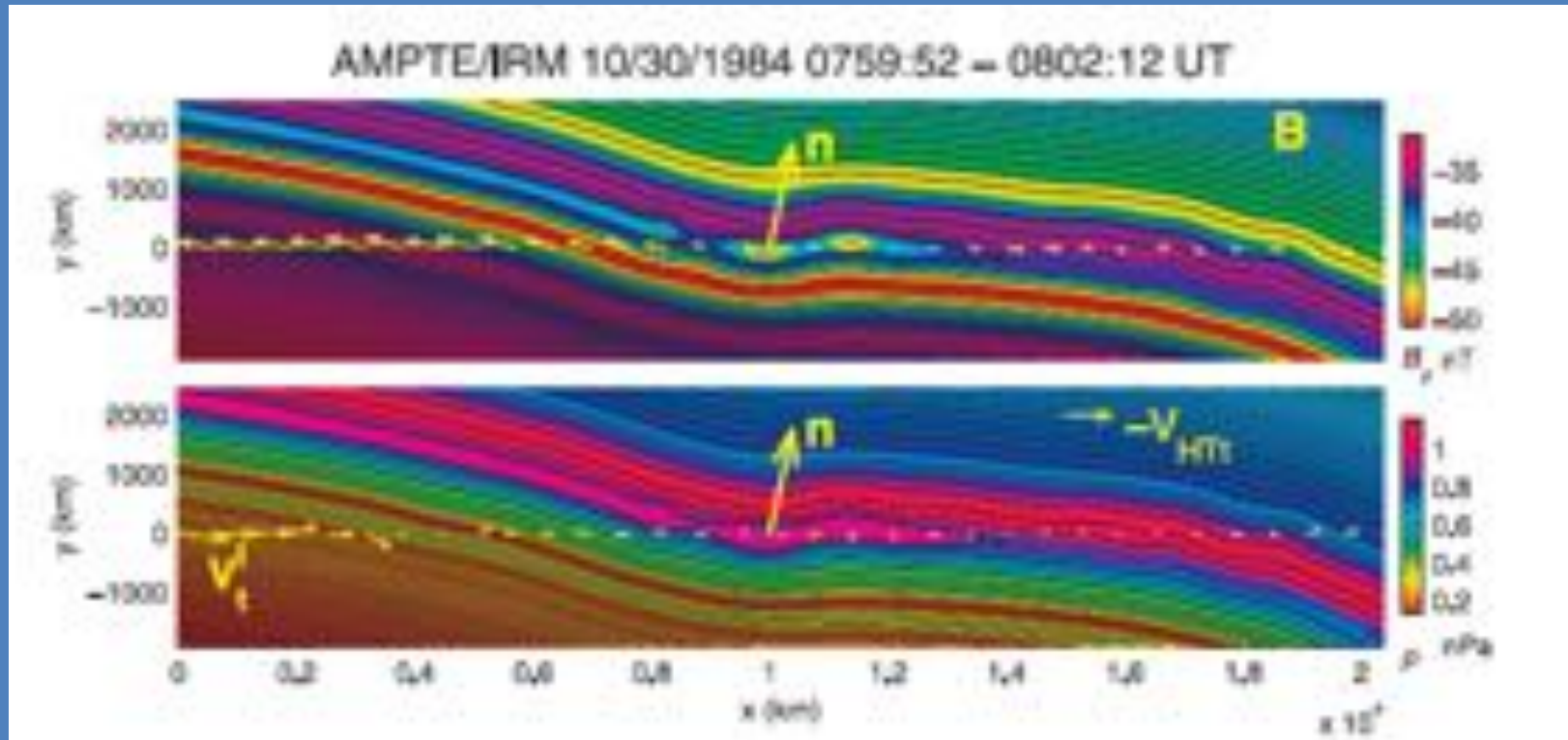
Results

AMPTE Oct 30, 1984

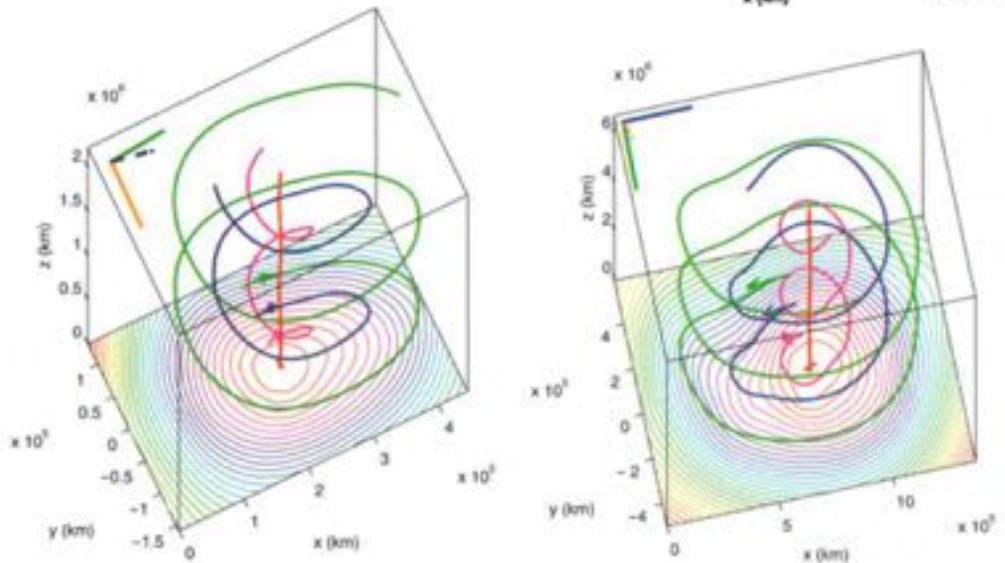
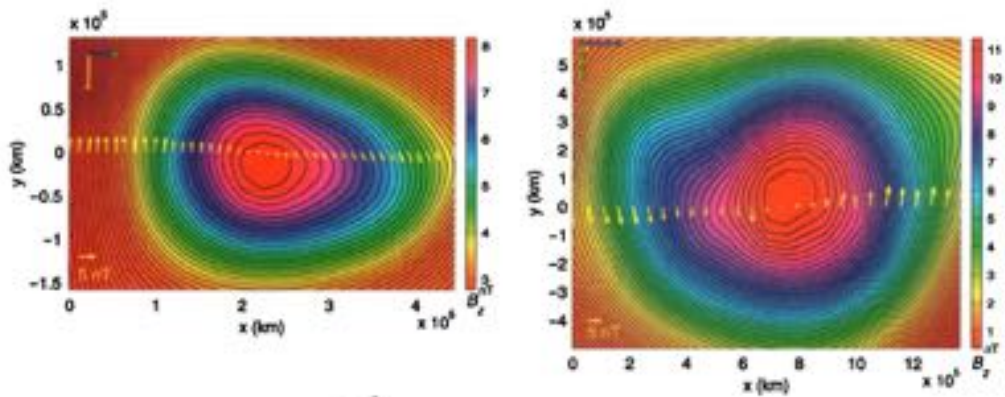
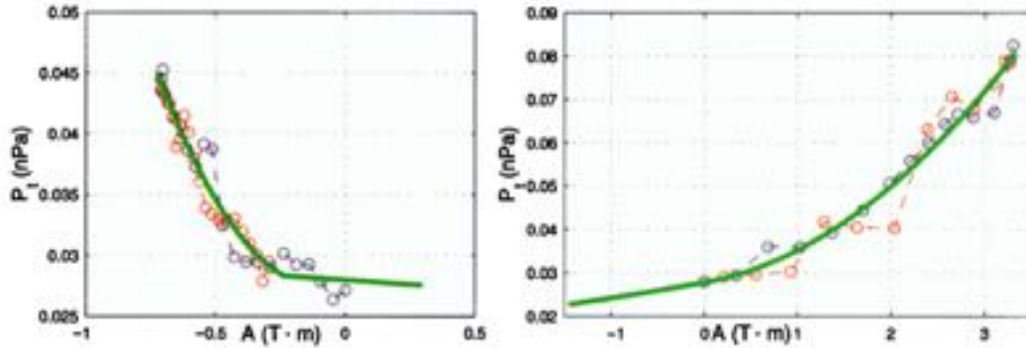


Hu and Sonnerup 2003

Results



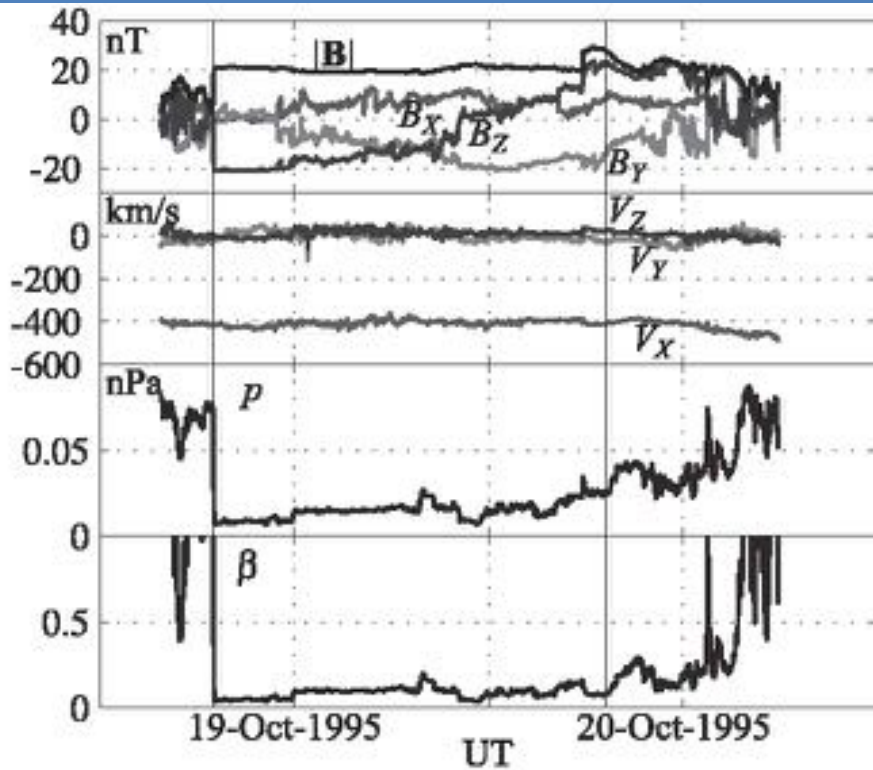
Results



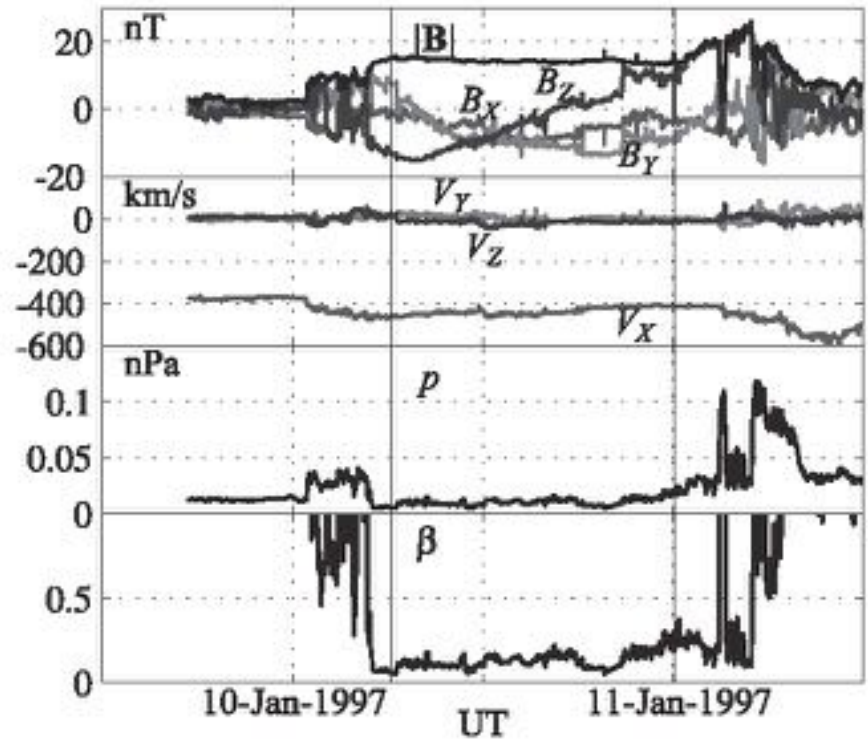
Reconstructed flux ropes for WIND May 2, 1996 (left) and March 13, 1996 (right) events.

Figures from Hu & Sonnerup 2001

Results



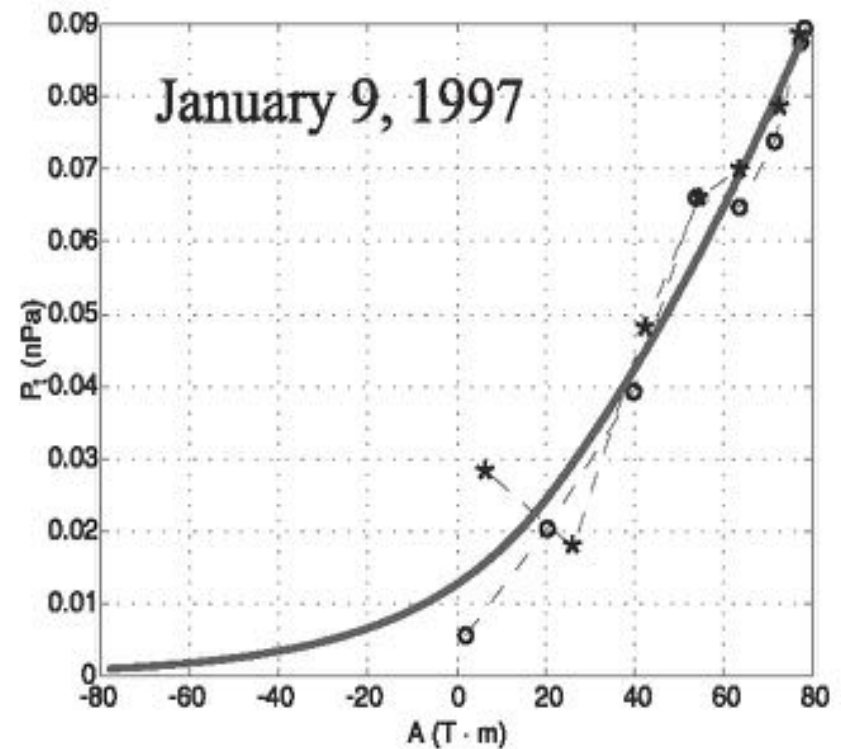
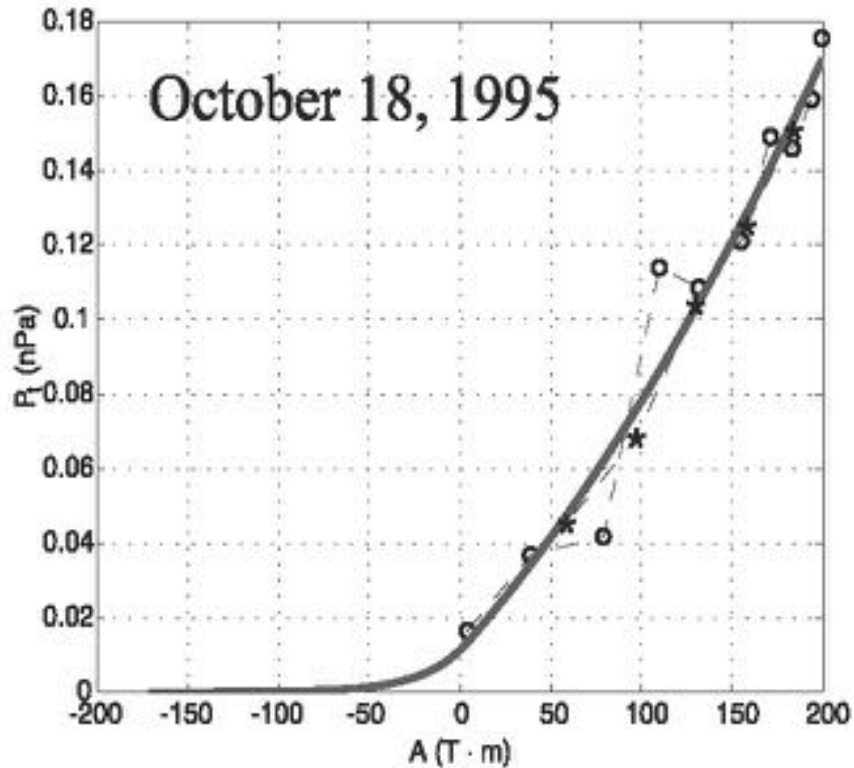
Time series of Wind 18 October 1995 magnetic cloud event



Time series of Wind 9 January 1997 magnetic cloud event

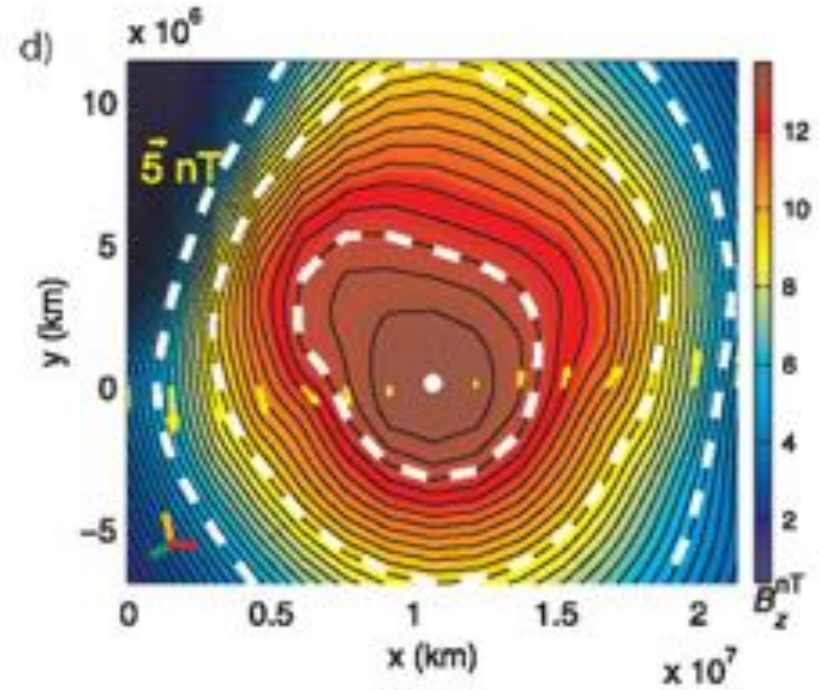
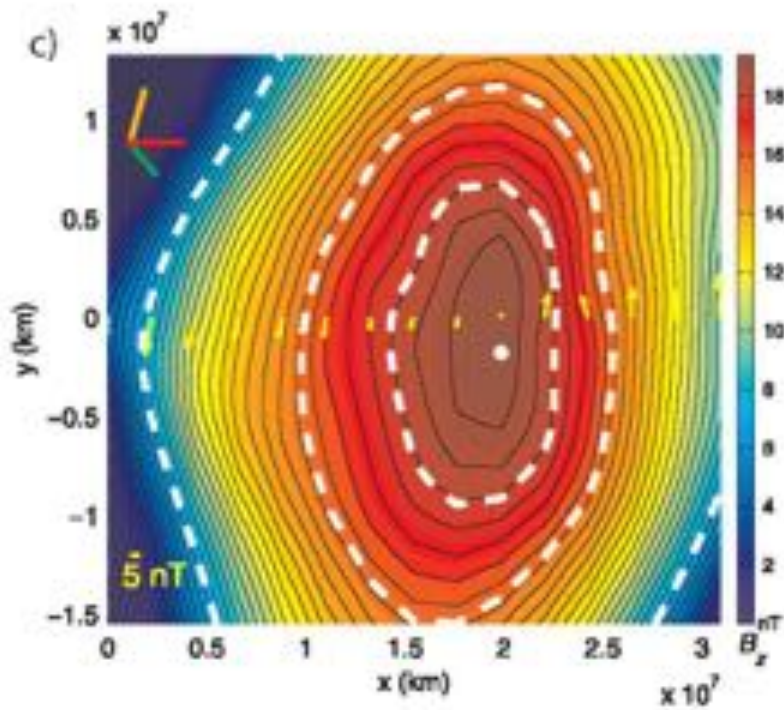
Figures from Hu & Sonnerup 2002

Results



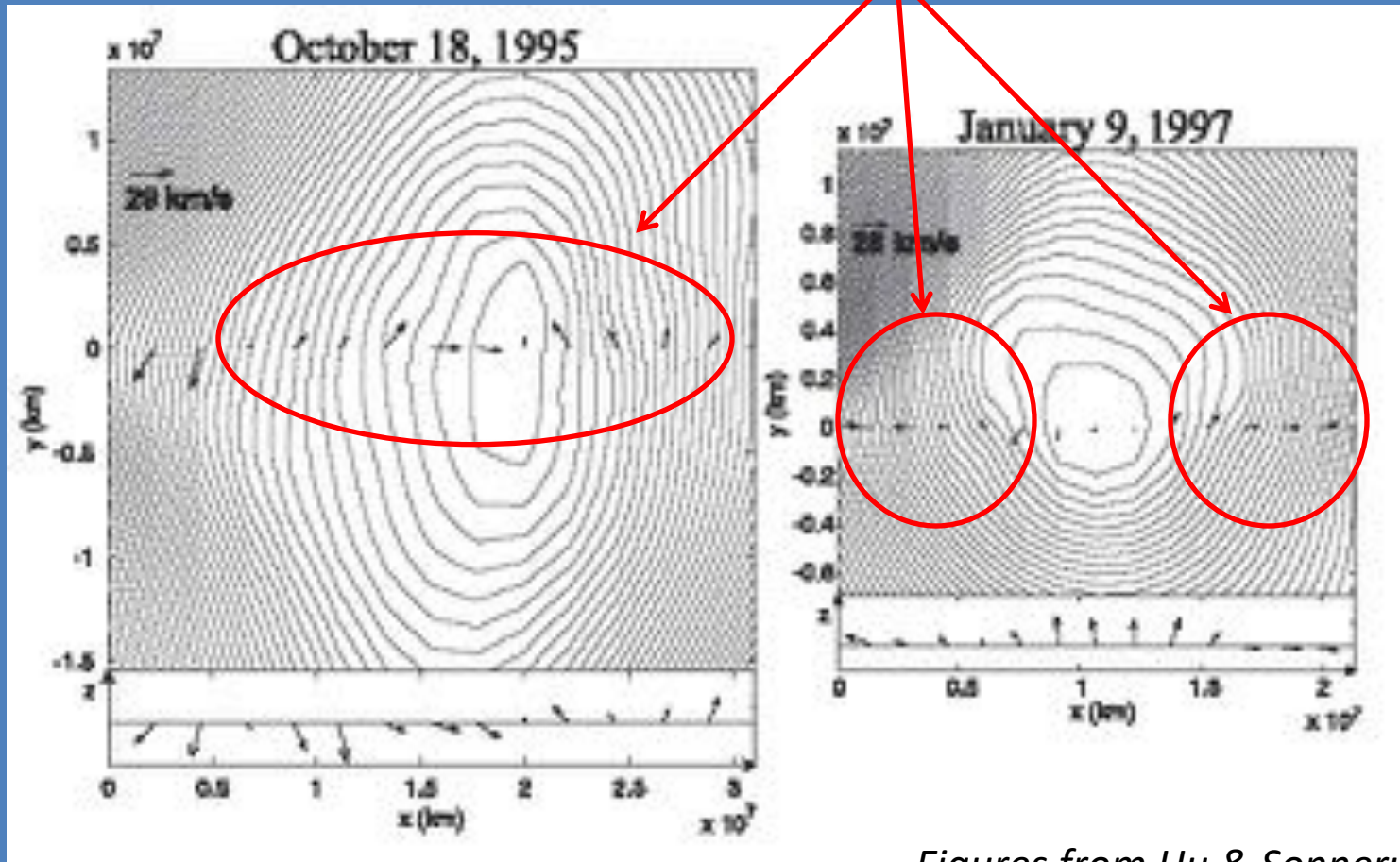
Figures from Hu & Sonnerup 2002

Results



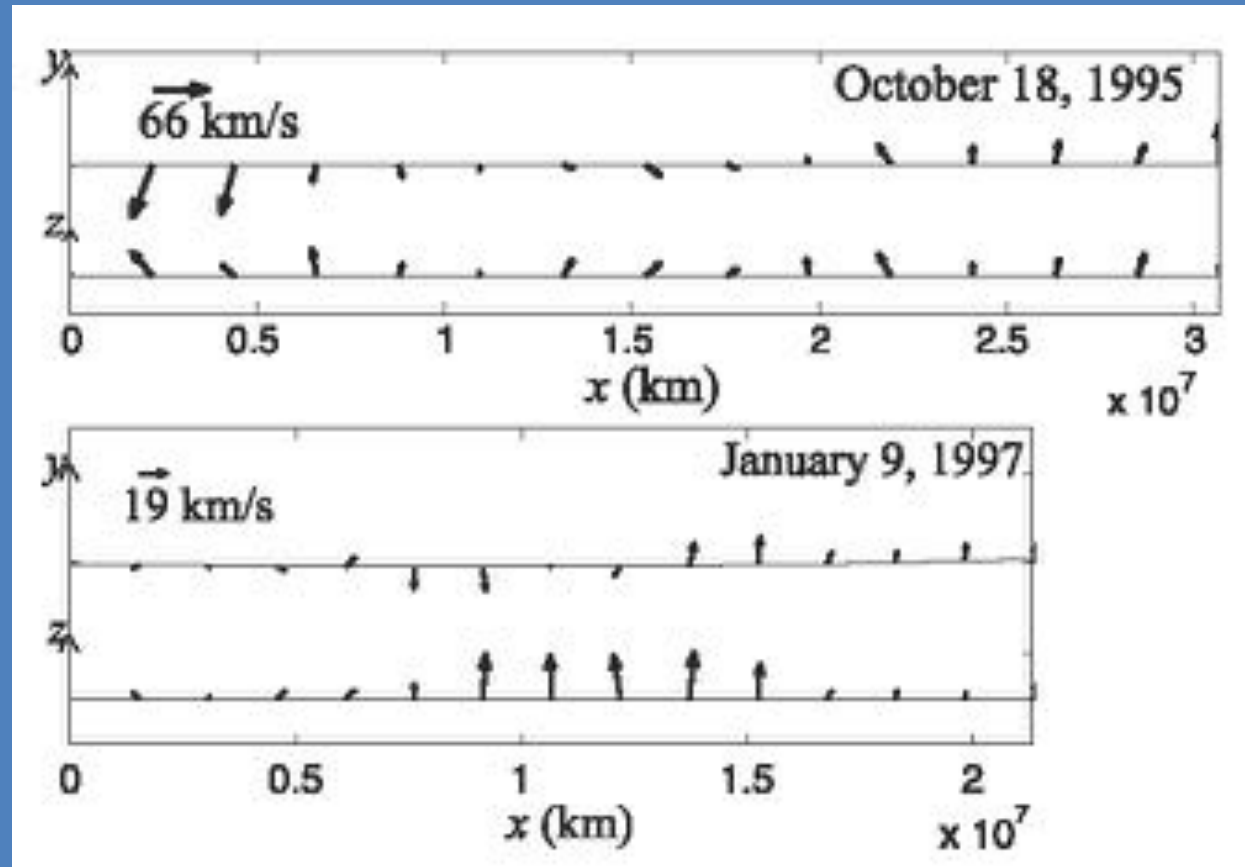
Figures from Hu & Sonnerup 2002

Results



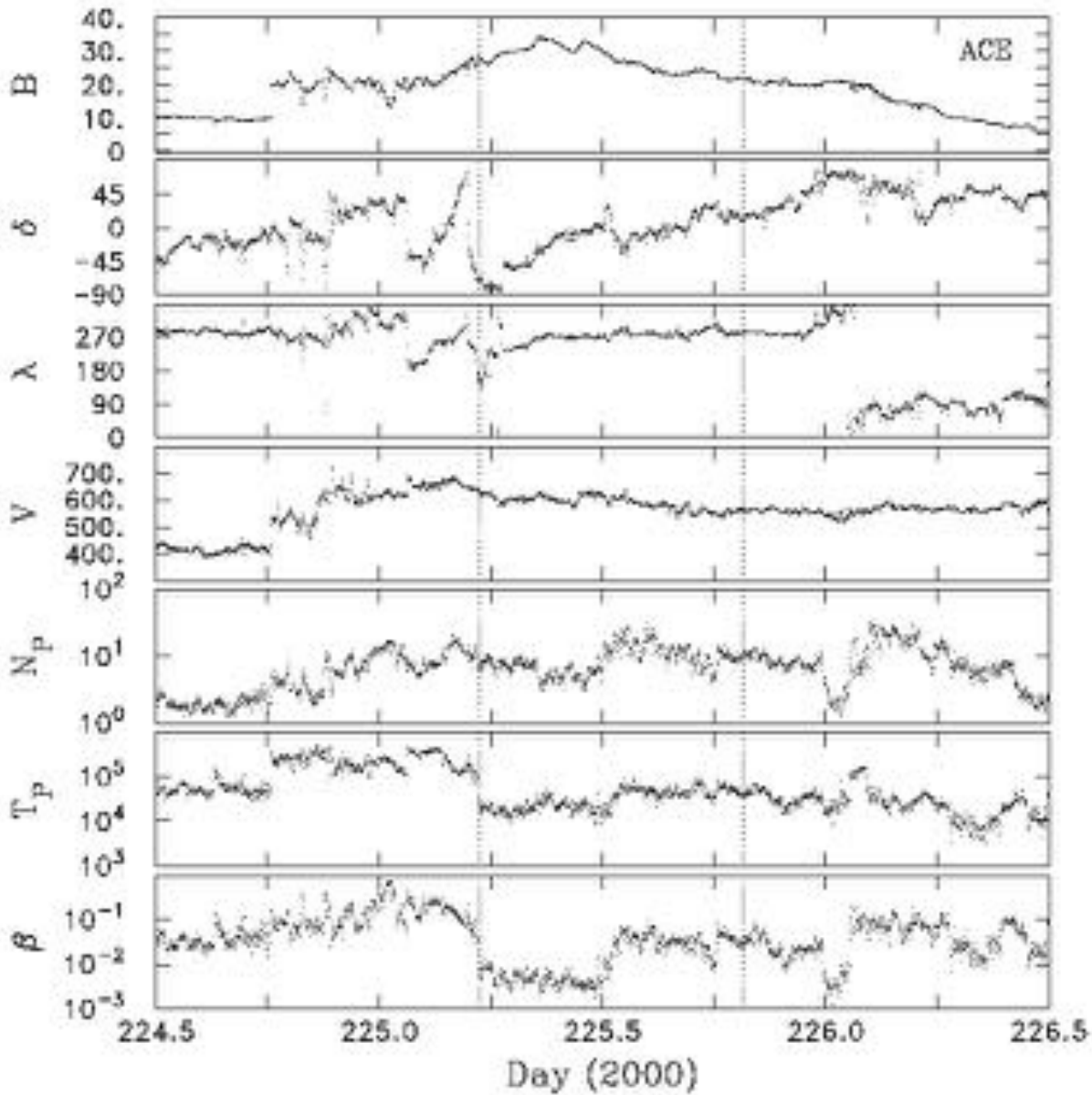
Figures from Hu & Sonnerup 2002

Results



Figures from Hu & Sonnerup 2002

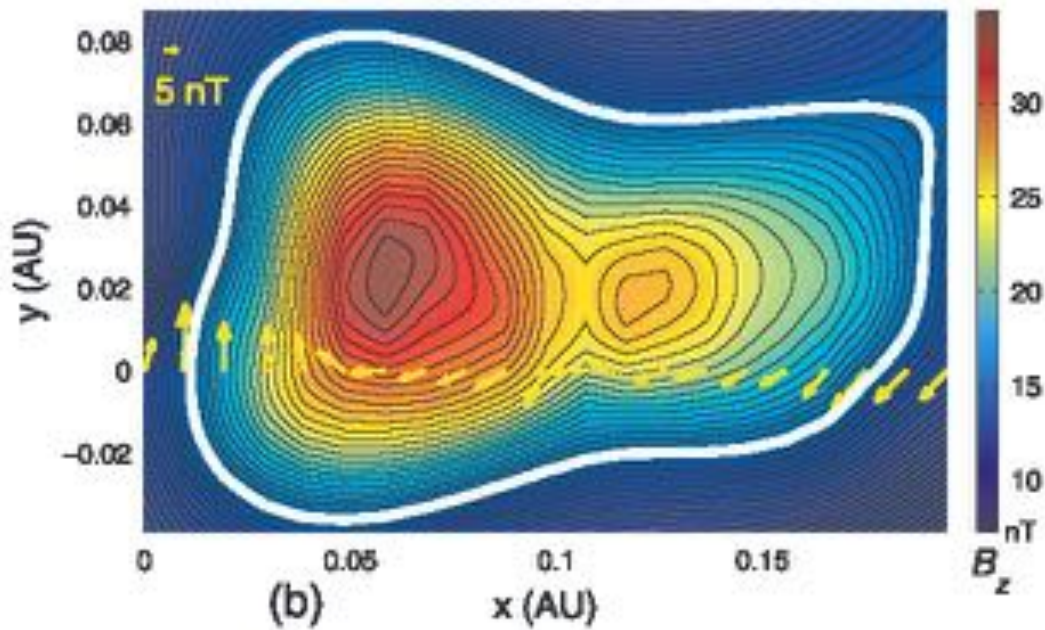
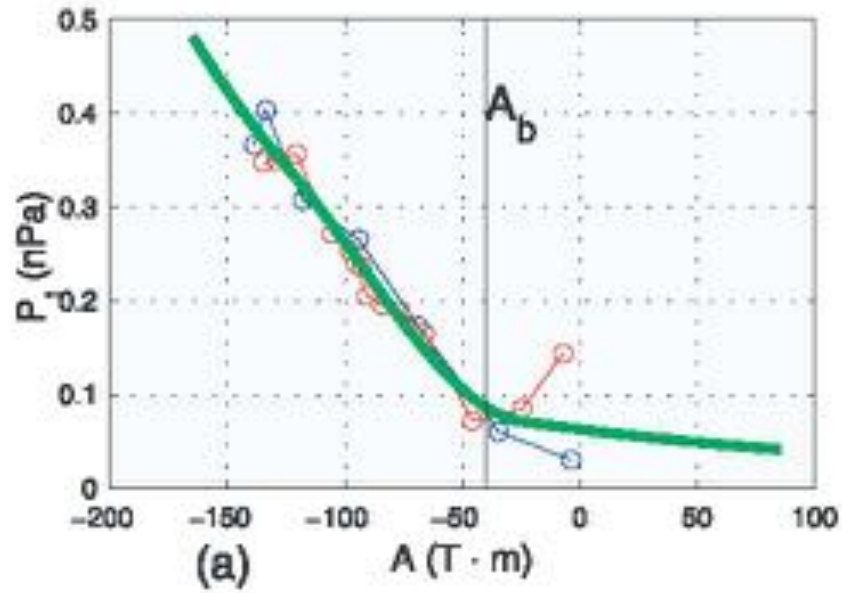
Results



ACE MAG and
SWEPAM
measurements on
August 12, 2000

*Figures from Hu
et al 2003*

Results

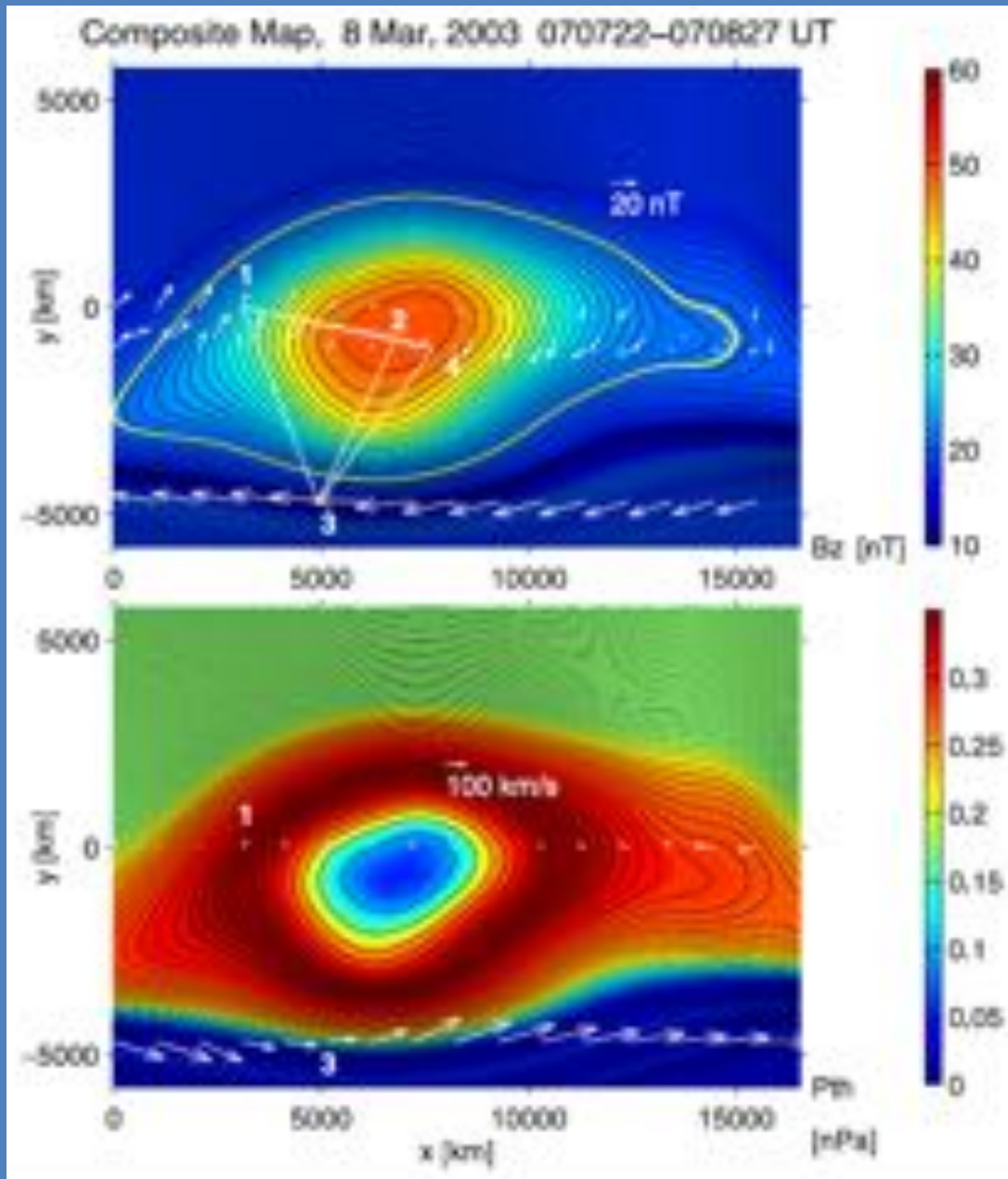


Figures from Hu et al 2003

Other Results

- Time Evolution of magnetohydrostatic Grad-Shafranov equilibria using single spacecraft data
 - Basic idea is to advance the set of spatial data before and after the actual spacecraft-data, then produce a series of field maps
 - i.e. do the time integration first, then the spatial integration
 - *Hasegawa et al 2010*
- Multi-Spacecraft
 - Cluster
 - Combined GSR field maps from all 4 spacecraft
 - *Sonnerup et al 2004*

Sonnerup et al 2004



*Figures from
Sonnerup et al 2004*

Limitations

WARNING!!!!

- Cannot be used for vortices with rapid temporal variation
- Numerical instabilities
- The maximum integration domain
- Availability of spacecraft plasma data
- Extrapolation and interpolation of data

That's all folks!!

Questions??